

14
LA-3384-MS

C.3

CIC-14 REPORT COLLECTION
REPRODUCTION
COPY

LOS ALAMOS SCIENTIFIC LABORATORY
of the
University of California
LOS ALAMOS • NEW MEXICO

The Molten Plutonium Burnup Experiment



UNITED STATES
ATOMIC ENERGY COMMISSION
CONTRACT W-7405-ENG. 36

LEGAL NOTICE

This report was prepared as an account of Government sponsored work. Neither the United States, nor the Commission, nor any person acting on behalf of the Commission:

A. Makes any warranty or representation, expressed or implied, with respect to the accuracy, completeness, or usefulness of the information contained in this report, or that the use of any information, apparatus, method, or process disclosed in this report may not infringe privately owned rights; or

B. Assumes any liabilities with respect to the use of, or for damages resulting from the use of any information, apparatus, method, or process disclosed in this report.

As used in the above, "person acting on behalf of the Commission" includes any employee or contractor of the Commission, or employee of such contractor, to the extent that such employee or contractor of the Commission, or employee of such contractor prepares, disseminates, or provides access to, any information pursuant to his employment or contract with the Commission, or his employment with such contractor.

All LA...MS reports are informal documents, usually prepared for a special purpose and primarily prepared for use within the Laboratory rather than for general distribution. This report has not been edited, reviewed, or verified for accuracy. All LA...MS reports express the views of the authors as of the time they were written and do not necessarily reflect the opinions of the Los Alamos Scientific Laboratory or the final opinion of the authors on the subject.

Printed in USA. Price \$3.00. Available from the Clearinghouse for Federal Scientific and Technical Information, National Bureau of Standards, United States Department of Commerce, Springfield, Virginia

LOS ALAMOS SCIENTIFIC LABORATORY
of the
University of California
LOS ALAMOS • NEW MEXICO

Report written: September 2, 1965

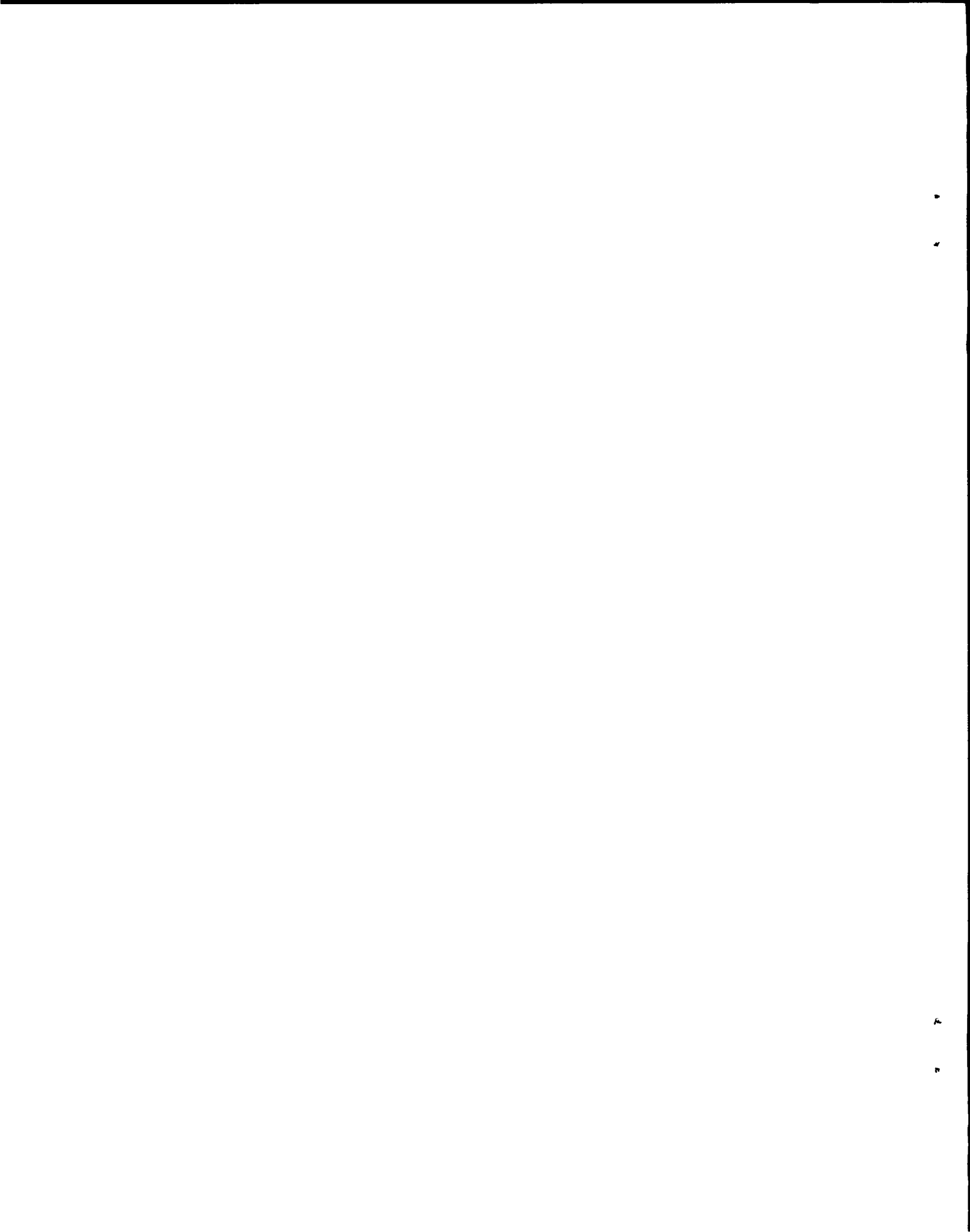
Report distributed: January 6, 1966

The Molten Plutonium Burnup Experiment

by

W. H. Hannum and L. D. Kirkbride



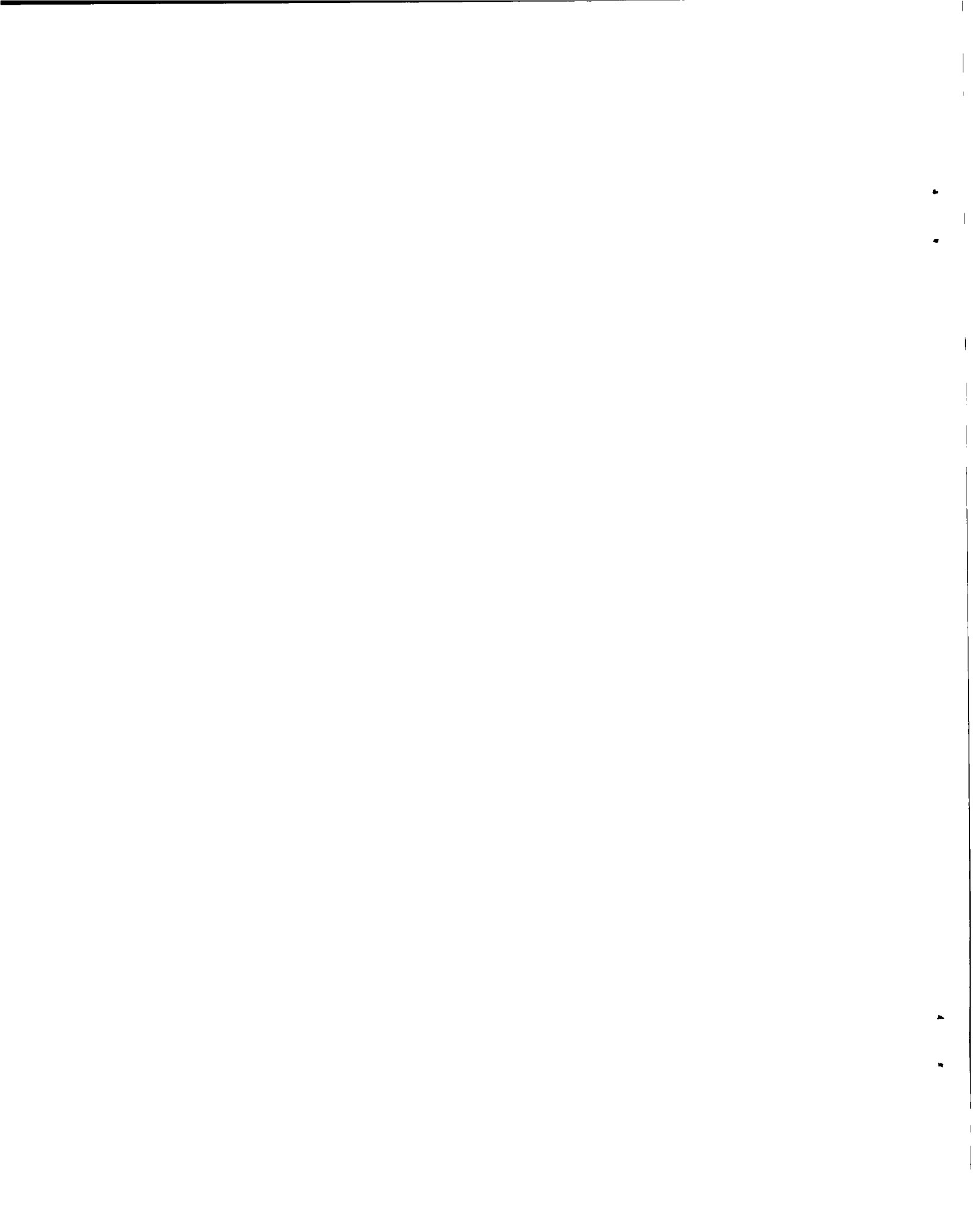


ABSTRACT

A reference core has been selected for a Molten Plutonium Burnup Experiment. In this experiment, the fuel, a Pu-Co-Ce alloy, will be contained in sealed Ta-W alloy capsules. The principal purpose of the experiment is to obtain information on the characteristics of molten-Pu fuel during and after high burnup at high rates of fissioning. Further data on nuclear, thermal, and materials performance of molten-Pu-fueled reactor systems will also be obtained. Present uncertainties prevent a detailed analysis or optimization of performance characteristics. Nevertheless, systems based on the use of this fuel alloy can reasonably be expected to have a very favorable fuel lifetime, short doubling time, and favorable safety characteristics. This experiment will be operated in the Los Alamos Fast Reactor Core Test Facility.

ACKNOWLEDGEMENTS

The material discussed here represents the work of many people. In particular, many of the nuclear generalizations and thermal performance optimizations are the work of G. L. Ragan. Detailed thermal analyses for the reference case were contributed by H. I. Bowers. The material data include experimental results obtained by G. E. Meadows, F. B. Litton, and others. The mechanical layout utilized is largely due to R. A. Clark and J. A. Bridge.



CONTENTS

	<u>Page</u>
ABSTRACT	3
ACKNOWLEDGEMENTS	3
1. INTRODUCTION	7
2. MOLTEN Pu AS A FAST BREEDER FUEL	9
2.1 Fabrication Charges (Lifetime Capability)	9
2.2 Fuel Costs (Doubling Time Estimation)	11
2.2.1 Breeding Ratio	11
2.2.2 Specific Power	15
2.2.3 Optimization for Capsule Core	16
2.3 Safety	16
2.4 Other Factors	18
3. CORE DESIGN PARAMETER SELECTION	19
3.1 Power Density	20
3.2 Facility Limits	22
3.3 Optimization	25
4. FUEL ELEMENT DESIGN	27
4.1 Container Alloy	30
4.1.1 Corrosion Performance	30
4.1.2 Mechanical Properties	33
4.1.3 Irradiation Properties	35
4.2 Fuel Alloy	40
5. CORE DESIGN MODEL	43
5.1 Region Compositions	43
5.1.1 Core	43

	<u>Page</u>
5.1.2 Reflector	43
5.1.3 Control Segments	45
5.1.4 Structure	48
5.1.5 External	48
5.2 Geometry	48
6. CALCULATIONAL RESULTS	51
6.1 Critical Size and Loading	51
6.2 Control Worths	52
6.3 Reactivity Coefficients	54
6.4 Core Parameters	54
7. APPLICATION TO LARGE POWER REACTORS	57
7.1 Core Parameters	57
REFERENCES	62
APPENDIX A - Doubling Time and Costing Factors	64
APPENDIX B - Neutron Balance	68
APPENDIX C - Thermal Performance Relations	70
APPENDIX D - Measures of Irradiation Times	73
APPENDIX E - Results of Pu-Co-Ce Alloy Corrosion Tests (Na Loop Environment)	75
APPENDIX F - Results of Pu-Co-Ce Alloy Corrosion Tests (Static Inert-Gas Environment)	76

1. INTRODUCTION

It has been recognized for some time that the use of a fluid reactor fuel has certain distinct advantages. Traditionally, these advantages have been identified as convenience in handling. More recently, it has been suggested that molten Pu as a fast breeder fuel has significant advantages in breeding gain, safety, and fuel lifetime. There may be further advantages in reprocessing, but this aspect is not discussed in the present analysis.

The operation of the 1 MW LAMPRE I⁽¹⁾ reactor has demonstrated (1) the basic feasibility of operating with a molten fuel in a sealed capsule, (2) the release of a large part (>80%) of the volatile fission products from the fuel to the contained gas space, (3) the stability of this type of system, and (4) the satisfactory containment of the fuel for extended periods of time. This operation has been described elsewhere.⁽²⁾

The Molten Plutonium Burnup Experiment (MPBE) is the next major experiment in the orderly development of molten-Pu fuel and of a breeder concept utilizing this fuel. The principal purpose of the experiment is to investigate the behavior of molten-Pu fuels during and after rapid and high burnup. In addition, operation of the core is expected to supply data on performance and operational characteristics of the core, including thermal, nuclear, and safety features. One feature of particular interest, as it affects both materials and nuclear properties, is the extremely hard neutron spectrum of such a system.

The general criteria which have been used in defining performance goals for the design of the experiment are those appropriate for a large-scale central power station application.⁽³⁾ The technology obtained in

this effort, however, is intended to be of such a depth that the applicability of molten-Pu fuel to other systems can be evaluated.

In the chosen reference design, the basic unit, or subassembly, is a stainless steel can containing seven fuel capsules. Each capsule is sealed and designed to positively contain both fuel and fission products. Thermal and mechanical designs are conservative with regard to stresses. The materials and operating parameters have been selected such that no significant failure rate of individual capsules is anticipated. The subassembly construction is such as to permit convenient sampling of capsules, insertion of special tests, and other fuel handling. The fuel is a ternary alloy (Pu-Co-Ce), contained in a Ta-5 w/o W (Ta-5W) alloy capsules. The core will be operated in the Los Alamos Fast Reactor Core Test Facility (FRCTF)⁽⁴⁾ which has a 20 MW heat removal capacity. Control will be exercised by a combination of moving fuel and peripheral poison, either of which will be adequate for emergency shutdowns.

In the sections which follow, the bases for interest in a molten-Pu fuel for central station applications are discussed; the selection of parameters for the MPBE are considered; the experimental basis for the selection of materials is presented; the reference core design is shown; performance estimates for the core are given; and the inferred performance levels for large core applications are considered.

2. MOLTEN Pu AS A FAST BREEDER FUEL

The interest in using molten Pu as a fast breeder fuel is based on its potential for safe and economic power generation. In discussing the bases for this interest, therefore, it is necessary to consider those factors which directly or indirectly affect the fuel cycle (or plant) economics. The question of realistic breeder fuel cycle economics, however, suffers from an almost complete ignorance of several important performance factors. Even for light water-moderated, oxide cores, the reliable estimation of fuel cycle costs is just now becoming feasible.

There are two factors in the fuel cycle costing, however, which are common to all reactors and which are frequently the dominant factors: fuel charges (burnup or buy-back, plus use charge), and fabrication charges.⁽⁵⁾ The fuel charges are reflected in the system doubling time (Appendix A), and fabrication charges are related to total burnup* capability of the fuel elements (per unit fabrication cost).

2.1 Fabrication Charges (Lifetime Capability)

Lifetime (burnup) capability for most fast reactor fuel elements is determined by structural damage to the fuel. With a molten fuel, no structural damage to the fuel itself can occur. Reactivity lifetime considerations can (conceptually) be avoided. The burnup limit is thus likely to be determined by fuel containment life, gross chemical fuel changes due to fission products, or simply by economics.

* Throughout this discussion, the term burnup will be used to refer to the total energy output (e.g., MWD) of an element, as is contrasted with burnup rate (power/element), fractional burnup (e.g., MWD/MT Pu), etc.

It is necessary, whatever the concept, to hold the fuel in some type of container, which may or may not be a heat transfer medium. In principle, the use of a fluid fuel permits changing of fuel without replacing the container. In practice, however, the container will have a finite lifetime. The lifetime of the container as compared with that of the fuel must be taken into consideration before deciding whether to refill or to replace containers. For a molten-Pu system, it is not clear whether the lifetime capability of the fuel or of the container (if either) will be limiting (Section 4). Thus, a decision as to whether to pursue a plumbed or a fixed fluid concept would be premature at this stage. It could be that the ability to handle fuel as a fluid will be more significant in the blanket than in the core.

There are several design concepts which have been considered for the molten-Pu system. The first, and perhaps most straightforward, is the sealed-capsule core. The core construction using such capsules is as it would be with a solid fuel. Heat generated in the fuel is transmitted through the container wall to the coolant stream. This is the type of fuel element which was used in LAMPRE I. The fission gas generated in the fuel is released to the contained gas space. The thermal performance of this type of element is, in general, limited by the heat flux through the container wall, either in terms of stress or in terms of the temperature of the fuel-container interface and hence corrosion. Fuel element lifetime may also be limited by the fission gas pressure buildup in the gas space.

A reasonable progression beyond the sealed capsule-type core is a design which avoids the pressure buildup by venting the fission gases, presumably to the coolant. More advanced concepts include systems in which the fuel and coolant are in direct contact or where the Pu is circulated for external gas disengagement, preprocessing, etc. (see, for example, Reference 6).

Since, without further experimental data, it is not possible to come to a quantitative defense of the systems which more fully utilize the

fluidity of the fuel, the present design uses sealed capsules and is compatible with the use of vented capsules. This selection of fuel container has several distinct practical advantages: the technology developed for solid fuel in thermal and mechanical designs is available and useful; the performance limits are more readily defined; a failure of containment has limited and tolerable consequences; and the design is well suited to collection of data on materials properties as a function of burnup. In addition, actual successful operational experience on such a core exists (LAMPRE I).

The principal purpose of the MPBE is to extend the available data on the properties of the fuel and, to some degree, the properties of Ta containers, during and after high burnup. Upon completion of this experiment, it may be feasible to define realistic burnup limits.

2.2 Fuel Costs (Doubling Time Estimation)

For any system, the doubling time may be expressed in terms of factors which are more directly measurable. To a reasonable approximation (see Appendix A)

$$DT = \frac{3}{(BR - 1) SP} , \quad (2.1)$$

where

DT = doubling time in years at $\approx 83\%$ load factor,

BR = atoms of fuel (e.g., fissile Pu) produced per atom of fuel lost,

SP = specific power in MW per kg of fuel in the inventory.

It is convenient (but not accurate) to consider here a beginning-of-life breeding ratio and an inventory equal to one beginning-of-life core loading.

2.2.1 Breeding Ratio

Breeding ratio may be expressed (Appendix B) as

$$BR = (\eta - 1) - a + b, \quad (2.2)$$

where

- η = neutrons born per neutron absorbed in fuel,
- a = neutrons lost to nonfuel parasites and leakage per neutron absorbed in fuel,
- b = net neutrons produced in fertile fissions per neutron absorbed in fuel.

Thus, high breeding ratio is obtained with high η and b and low a .

To obtain a high η for the reactor, it is desirable to use Pu rather than U as a fuel, and to use it in as hard a spectrum as feasible. This fact is illustrated by the data of Fig. 2.1. The hard spectrum is characteristic of a metal fuel in preference to a ceramic. In addition, the fast fission in U-238, and thus factor b in Eq. (2.2), is high for hard spectra. Thus, the molten-Pu system has good breeding potential [$\eta \approx 2.7$ as compared with 2.2 in a ceramic fast breeder⁽⁷⁻¹⁰⁾].

The breeding ratio is largely determined by η and by the ratio of parasitic material content to Pu density in the core. Calculations have been done for a series of possible molten-Pu-fueled, sealed Ta-capsule-type 1000 MW(th) reactors, each composed of an array of modular cores. In this series, each modular core is 30 cm high, has 30-cm-thick axial blankets above and below, and has a 30-cm-thick radial blanket -- all blankets are UC_2 . The calculated breeding ratios are shown in Fig. 2.2 for several leakage assumptions. Curve 1 is closest to cases of practical interest, though the leakage may have been somewhat high, due to the use of thin carbide blankets. Other calculations shown in Fig. 2.2 (curve 4) are at the other extreme with regard to leakage, i.e., very low leakage because of the use of thick (45-cm) U-metal blankets. In all of these calculations, the Ta capsule material is the only substantial parasite. These calculations span a considerable range of designs and calculational models. Variations include

- (a) shape differences -- one set is for a series of cylinders of constant (30-cm) height, whereas, another set is for spheres;
- (b) spectrum effects -- curve 1 is for a carbide blanket, so should give a softer spectrum than did the U-metal blankets for curve

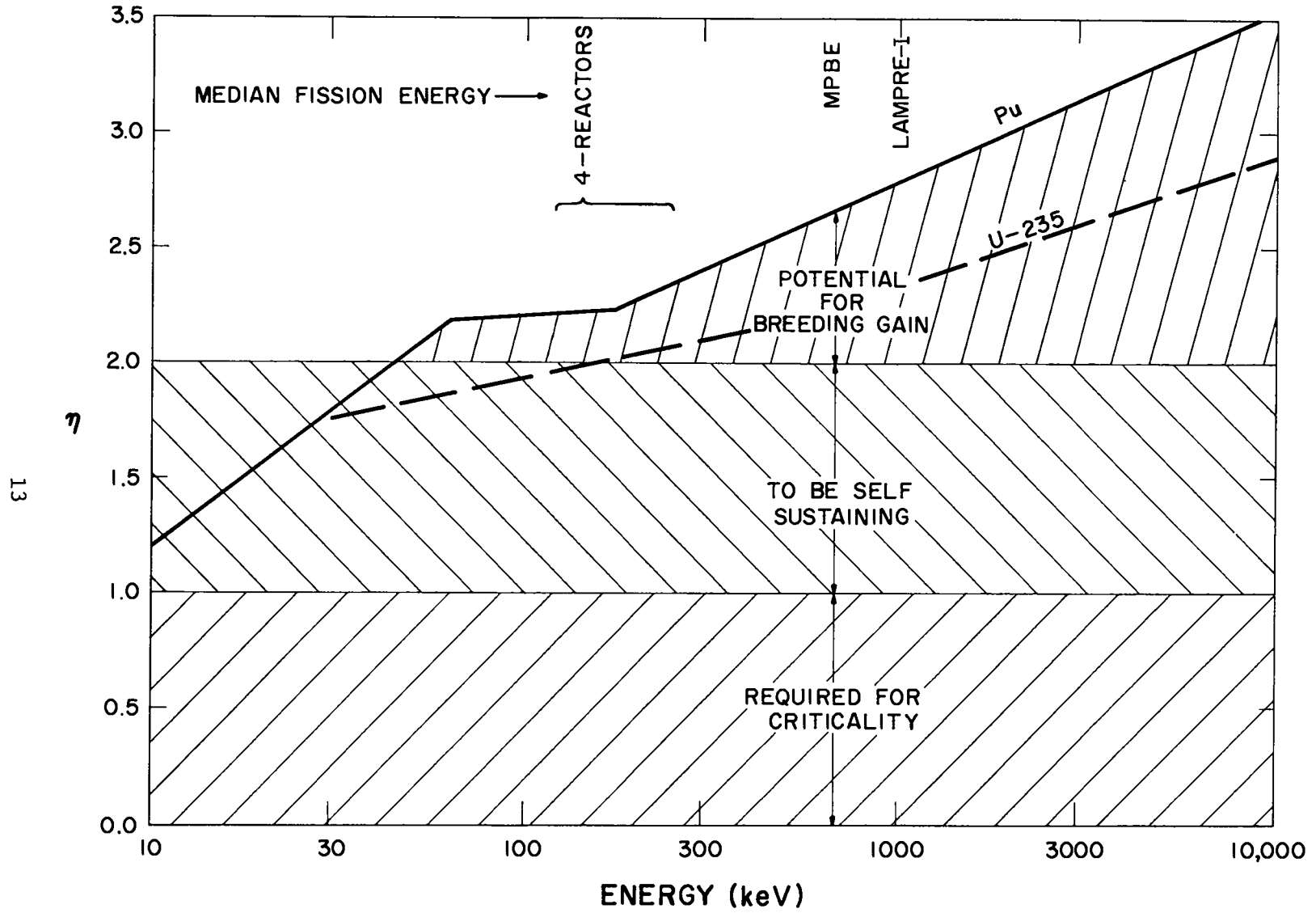


Fig. 2.1. Trend of $\eta(E)$ with E

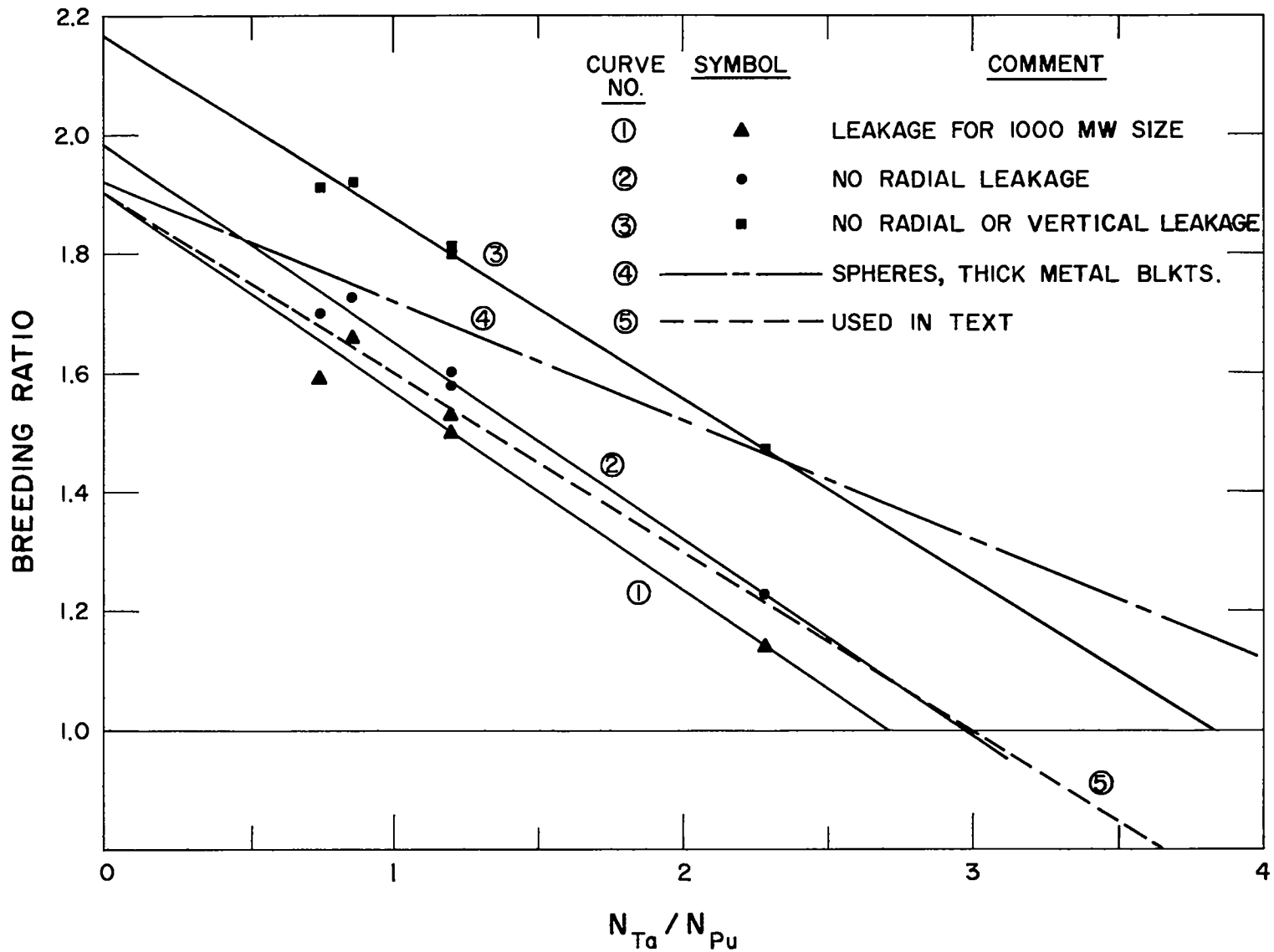


Fig. 2.2. Breeding Ratio as a Function of the Ratio of Ta to Pu Atoms

4. This tends to enhance the vertical leakage of the more dilute (higher Ta/Pu) systems, relative to the less dilute ones to the detriment of BR for the higher values of (Ta/Pu);

- (c) cross-section library -- curves 1 through 3 are for calculations using the Hansen-Roach 16-group set,⁽¹¹⁾ while those for curve 4 use Kiehn's 10-group set.⁽¹²⁾

Nevertheless, the compromise relation (curve 5), drawn slightly above curve 1 at the higher (Ta/Pu) end, may be considered as a reasonable generalization for all of these calculations. Based on this generalization, the BR for a Ta-capsule core may be expressed as

$$BR \approx 1.9 - 0.3 (Ta/Pu). \quad (2.3)$$

2.2.2 Specific Power

For a molten-Pu system, the criteria for obtaining high specific power are, in general, less well defined than are those for breeding ratio. Present emphasis is on systems in which the container material serves as a heat transfer medium (i.e., a capsule-type core). For this type of molten-Pu core, specific power will generally be limited by heat transfer capability (either in terms of stress or in terms of increased corrosion rates associated with an increased inside wall temperature associated with a high radial ΔT). For a fixed wall thickness, it is clear that the heat transfer area of the core is proportional to the total number of Ta atoms in the core. If the heat transfer is limiting, the specific power is then given by

$$SP \propto \frac{\text{core power}}{\text{Pu atoms in the core}} \propto \frac{\text{Ta atom}}{\text{Pu atom}} \equiv \frac{\text{Ta}}{\text{Pu}}. \quad (2.4)$$

Thus, specific power is increased by decreasing Pu per unit heat transfer area.

2.2.3 Optimization for Capsule Core

The preference for high (Ta/Pu) from Eq. (2.4) (so as to have high heat transfer area) is counter to that for low (Ta/Pu) from Eq. (2.3) (so as to have high BR), suggesting a compromise. In fact, substituting Eqs. (2.3) and (2.4) into Eq. (2.1) yields

$$DT = \frac{\text{const.}}{[0.9 - 0.3 (Ta/Pu)] (Ta/Pu)} \quad (2.5)$$

which clearly has an optimum for minimum DT, at (Ta/Pu) 1.5.

The attainment of a specified ratio (Ta/Pu) requires that, for a given Ta capsule wall thickness b and outside radius a , the Pu content of the fuel should be

$$\rho_f [\text{g Pu/cc fuel}] = \frac{43.3 b}{(Ta/Pu)(a - b)} \left\{ 1 + \frac{b}{2(a - b)} \right\}, \quad (2.6)$$

as shown in Appendix C.

For example, for $b = 0.025$ in., the fuels corresponding to a value (Ta/Pu) = 1.5, for several capsule outside diameters, are

o.d. [in.]	0.2	0.3	0.4	0.5	0.6
ρ_f [g Pu/cc fuel]	11.4	6.4	4.5	3.4	2.8

2.3 Safety

The use of molten-Pu alloy fuel has several unique and significant safety advantages, relative to the use of a solid ceramic fuel. A dominant factor is the fact that the fuel is liquid metal, with a substantial thermal expansion coefficient. Since the reference container material (a Ta alloy) has a very low coefficient of thermal expansion, the effective expansion of the liquid in a tube is almost three times that even of the corresponding solid metal. Thus, a large negative temperature coefficient is assured.

There is a second area with regard to safety in which these systems have a natural advantage. The molten-Pu/Ta system characteristically has an extremely hard neutron spectrum. This is necessary so as to avoid an excessive penalty from Ta parasitic capture. As has been pointed out (Section 2.2.1), there are also strong benefits in η and fast fission effect from this hard spectrum. This spectrum is maintained, however, only by neutronically decoupling, to some degree, the U-238 from the Pu. Thus, a totally external breeder is the natural configuration. A high total power system is obtained by a system of multiple, loosely coupled core-blanket reactor modules.⁽³⁾ The system, even for large power station application, thus has very high leakage and a very hard spectrum.

An accident consideration which is frequently troublesome for large fast breeder power reactors is Na voiding. The Na void effect is a result of the balance between changes in leakage, Na parasitic capture, and Na moderation.⁽¹³⁾ A qualitative balance of these factors for several concepts is shown as Table 2.1. The modular arrangement, with high or total external breeding, may be desirable with ceramic fuels also.⁽¹⁰⁾

Table 2.1

Qualitative Na Void Effect Factors

<u>Factor</u>	<u>Type of Change on Loss of Na</u>	<u>Reactivity Effect In</u>		
		<u>Ceramic Fuel</u>	<u>Ceramic Fuel in Softened Spectrum</u>	<u>Molten Pu in Modular Array</u>
Core Leakage	Increase	Slight Neg.	Slight Neg.	Strong Neg.
Na Parasite	Loss of Parasite	Pos.	Large Pos.	Slight Pos.
Na Moderation	Increase η (Pu)	Pos.	Pos.	Slight Pos.
Net Effect	---	Pos.	Pos.	Strong Neg.

A further area of difference with regard to safety is in the Doppler effect. The net Doppler effect is again a balance between a negative component (U-238) and components which are presumably positive (Pu-239). While no quantitative advantage can be listed for the molten-Pu system, the Pu component (which is presumably positive) is totally negligible, due to the hard spectrum. The U-238 contribution, while perhaps reduced for some accidents by the neutronic decoupling, certainly is still negative. With the present uncertainties in prediction of Doppler effects, there are definite advantages to a system in which one is assured of the sign of the Doppler effect and not dependent on its magnitude.

Another potential safety advantage to the molten-Pu concept for a large fast breeder central station application is in fission product inventory. It may be possible and useful to use the fluidity of the fuel to obtain a partial continuous removal of fission products.

2.4 Other Factors

There are other features of a molten-Pu system which may differ from other fast breeders, such as existence of a minimum acceptable temperature and low equilibrium Pu-240 content.

It should be pointed out that some of the presently envisioned advantages to such a core concept depend to some extent on the fact that the blanket has a low multiplication. Since all Pu production is in the blanket, this implies a need for careful attention to blanket cycling.

In such systems, there is a large range of temperature in excess of normal operating temperatures which, for short times, is quite acceptable. For example, in the reference core, the first phase change is Na boiling. To obtain even local boiling requires an increase in Na temperature of more than 200°C. No bulk phase change in the fuel can reasonably be obtained with the high boiling point and sealed containment.

3. CORE DESIGN PARAMETER SELECTION

The MPBE is designed to supply additional data on the characteristics of molten-Pu fuel during high burnup. In addition, it is hoped that the experiment will supply early answers to some of the practical problems of large molten-Pu-fueled systems.

The performance potential of a molten-Pu system will clearly be affected by burnup in many ways. For example:

- (a) The change in Pu content by burnup will change the physical character of the fuel (melting point, etc.).
- (b) The presence of gross fission products may affect the fuel containment problem.
- (c) The volatile fission products will cause a pressure buildup in sealed capsules.
- (d) The rate of gas generation will affect the equilibrium dilution (bubble content) of the fuel (the detailed character of this dilution at high burnup is not known).
- (e) The presence of insoluble fission products may result in mechanical changes to fuel performance (e.g., interference with natural convection in the fuel).

For ceramic fast reactor cores, a burnup of $\approx 10\%$ of the heavy atoms is currently used as a design point.⁽⁷⁻¹⁰⁾ For solid metallic fuels, the present limit is less.⁽¹⁴⁾ It seems unreasonable to consider less than 10% burnup to be a design goal for a molten-metal pin-type core, nor are there known reasons to expect less.

With regard to these considerations, we may inquire as to the parameters which are to be optimized in the design. It may be noted that power is fission or burnup (absolute) rate, specific power (power per unit Pu) is fractional burnup rate (depletion rate/atom), and power

density is burnup rate/unit volume. Therefore, fractional burnup (integrated specific power) is a reasonable measure of flux time (nvt) (Appendix D). The change in neutronic properties is likely to be described in terms of fractional burnup -- or integrated specific power. For container irradiation damage, integrated specific power is the factor of interest. Fuel changes are more likely to be characterized by gross fission product content, i.e., integrated power density.

Since the present experiment is principally directed toward investigations of fuel behavior, the emphasis in the design is on power density to the extent that there are reasons to differentiate between power density and specific power. This separation relies on the assumption that Pu density and the effects of burnup are not strongly related.

3.1 Power Density

Several generalizations may be helpful in estimating power density limits for various configurations which have been proposed. The basis of these generalizations is the observation that, over an extended range, the critical mass for a capsule core can be simply related to the average Pu density. Figure 3.1 shows a plot, for a variety of cores, of the calculated critical loading as a function of average Pu density. As can be seen from the figure, all of these calculations can be reasonably fitted by the curve,

$$\text{loading [kg Pu]} = 270 \left(\bar{\rho}_f [\text{g/cc}] \right)^{-1.3} . \quad (3.1)$$

While other factors, of course, influence the loading (such as Ta content), in the region of particular interest, the relationship (3.1) is a reasonable generalization. The average fuel density, as used here, is

$$\bar{\rho}_f = \rho_f [\text{g Pu/cc fuel}] \cdot V_f [\text{cc fuel/cc core}] . \quad (3.2)$$

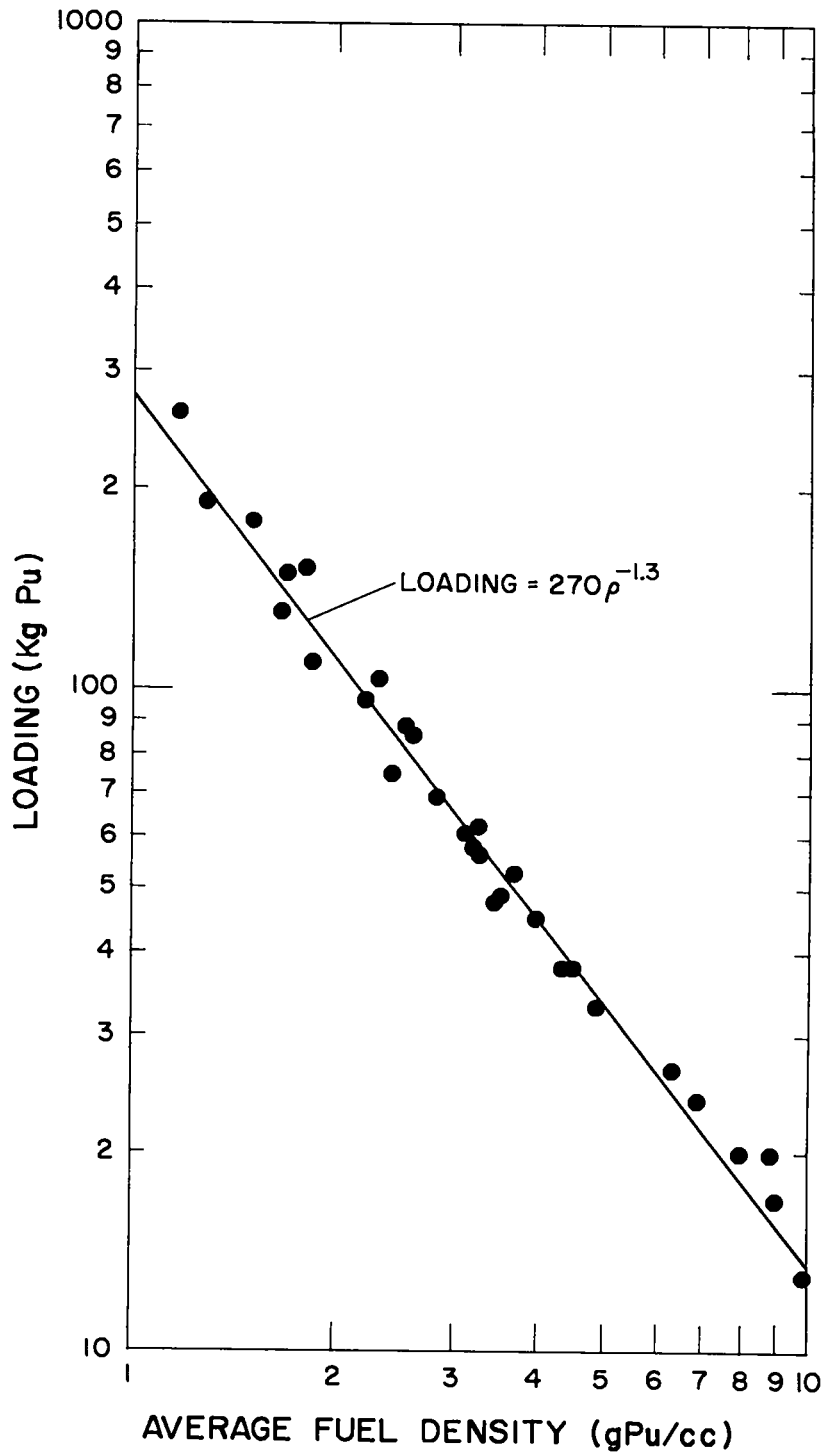


Fig. 3.1. Critical Loadings for Various Molten-Pu-Fueled Cores

A second relationship which is used here is the definition of power density. This may be written

$$PD = \frac{\text{power [MW(th)]} \cdot \text{density} \left[\frac{\text{kg Pu}}{\text{liter}} \right]}{\text{loading [kg Pu]}} \quad (3.3)$$

Combining these gives

$$PD \left[\frac{\text{MW}}{\text{liter}} \right] = \frac{P[\text{MW}] (\rho_f)^{1.3} [\text{g/cc}] (V_f)^{1.3} \cdot \rho_f}{270}$$

$$= 3.7 \cdot 10^{-3} P[\text{MW}] (\rho_f)^{2.3} (V_f)^{1.3} \quad (3.4)$$

3.2 Facility Limits

In discussing the parameters for the MPBE, it is also necessary to consider the limitations of the FRCTF. There are two principal limits which are significant here:

Power \lesssim 20 MW(th) (heat dump and heat exchanger limited)

Flow \lesssim 2500 gpm (pump and heat exchanger limited)

These two facility limits do, in fact, represent performance limits. The power limit enters from Eq. (3.4). Thus, in addition to the limitations associated with a large core application, there is also a limit on specific power and power density which increases monotonically with fuel density. Figure 3.2 shows some illustrative values of these limiting specific powers and power densities for various fuel densities. In a practical sense, of course, heat transfer capability and fuel containment limits also must be applied.

The second facility limitation (total flow) when combined with a temperature limit also presents a limitation. This can be seen from a simple temperature balance,

$$T_{\text{interface}} = T_{\text{inlet}} + \Delta T_{\text{Na}} + \Delta T_{\text{transverse}} \quad (3.5)$$

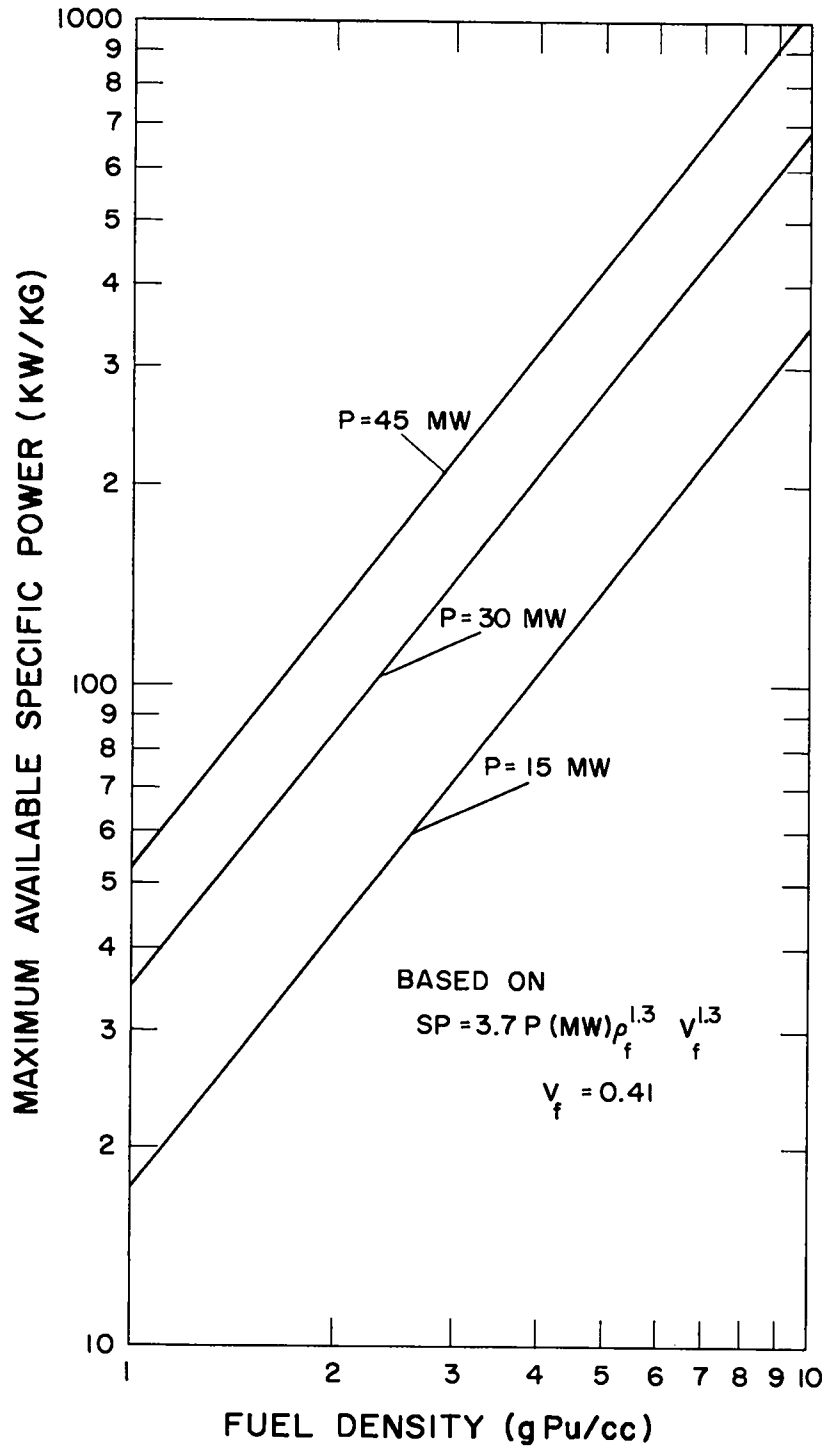


Fig. 3.2. Maximum Specific Power as a Function of Pu Density, Assuming Power Limited Operation

where

$T_{\text{interface}}$ is the fuel-Ta interface temperature in a typical channel,
 T_{inlet} is the Na inlet temperature,
 ΔT_{Na} is the mixed-mean Na temperature rise,
 $\Delta T_{\text{transverse}}$ is the temperature drop across Ta and Na film.

Inlet temperature is set at 480°C to avoid freezing of the fuel; and with 2500 gpm flow, the mixed-mean temperature rise at 20 MW is ≈120°C. The hot spot interface temperature limit is selected as 700°C (Section 4.1.1). Assuming that a 30°C peak-to-typical channel difference can be maintained, this allows 70°C for $\Delta T_{\text{transverse}}$. This is related to a heat flux by way of

$$\Delta T_{\text{transverse}} = \text{HF} \cdot t/k, \quad (3.6)$$

where

HF is the heat flux,
t is the wall thickness,
k is the wall conductivity.

For a 0.022-in. Ta wall ($k \approx 0.68 \text{ W/cm}^\circ\text{C}$), this implies an average channel heat flux of

$$\text{HF} \leq 850 \text{ W/cm}^2. \quad (3.7)$$

This may be related to an induced thermal stress, using

$$\text{stress} \approx \frac{E \alpha \Delta T}{2(1 - \nu)} \quad (3.8)$$

where

E is the elastic modulus,
 α is the linear thermal expansion coefficient,
 ν is the Poisson ratio for the container.

This gives, for a 70°C ΔT ,

$$\text{stress} \approx 9000 \text{ psi.} \quad (3.9)$$

Present understanding of the properties of Ta (Section 4) indicates that the 70°C ΔT will be a more restrictive limit than the 9000 psi induced thermal stress. The interface temperature limit (700°C) thus represents a heat transfer area lower limit. Any further reduction in heat transfer area must be compensated by a reduction in power in order to lower $\Delta T_{\text{transverse}}$ and the mixed-mean temperature rise.

3.3 Optimization

There are several ways in which the interplay between heat transfer area, power, and available fuel density can be described. For example, Fig. 3.3 shows the results of a study in which wall thickness, pitch/diameter, and interface temperature were held fixed, for various fuels and pin diameters. On this figure, it may be noted that points corresponding to power greater than 20 MW must be penalized by the 20 MW power limit. Further, no significant containment data are available for fuel densities above 8 g Pu/cc fuel. Based on this set of criteria, a capsule diameter of 0.420 in. has been selected for the MPBE. Since containment information is at present incomplete, a design compatible with either 6.2 or 8 g Pu/cc fuel has been selected.

Two factors should be reiterated with regard to the present design cases: First, the available performance levels are limited by the facility capability; and second, there is an interest in 8 g Pu/cc fuel (or higher), based solely on testing limits, and not on its particular applicability in a large system. (The eutectic at 12.1 g Pu/cc fuel would offer interesting testing possibilities, if feasible.)

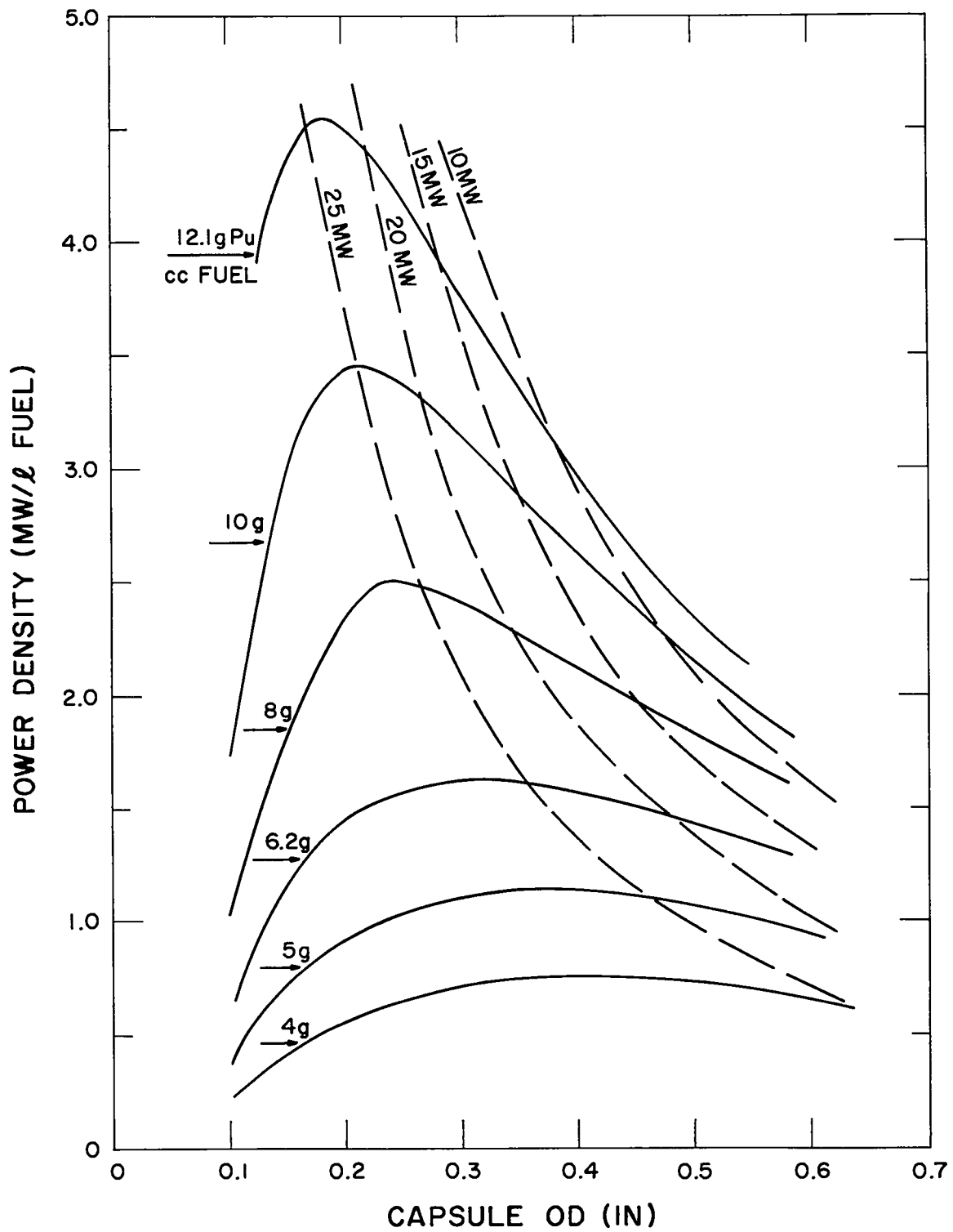


Fig. 3.3. Potential Power Density for MPBE Cores

4. FUEL ELEMENT DESIGN

In LAMPRE I, as in out-of-pile experience, the principal problem in utilizing a molten fuel has been that of finding a practical container. For Pu-rich fuels, Ta and Ta-W alloys appear to be the only possibilities among the many that have been tested.*

In the temperature range of interest for molten-Pu-fueled power reactors, i.e., 450-750°C, the Pu attack on Ta is by means of intergranular penetration (IGP). Pu penetration occurs by grain boundary diffusion in the Ta and eventually reaches the external surface of the containment causing a "failure." "Failure," in the present context, is defined as the presence of a detectable amount of Pu on the surface of a capsule after corrosion testing. The reliable detection limit for Pu is approximately 500 alpha cpm or $<10^{-8}$ g Pu.** (Most failures observed in test are less than 2000 cpm.) Even employing this stringent definition of failure, it normally takes many thousands of hours of testing with Pu-Co-Ce fuels before Pu penetration is detected (Appendices E and F).

A further area of concern is the expansion of the fuel on freezing. The Pu-Co-Ce alloys have volumetric expansions of 1-3% on freezing (Fig. 4.1). There are three potential solutions to this difficulty. First, an attempt has been made to modify this expansion characteristic by means

* There is some evidence, although quite preliminary in nature, that Nb or other refractory metals may be satisfactory for fuel of low Pu density, i.e., 10 a/o Pu.

** It is obvious this definition of failure is quite conservative with respect to failures of operational consequence in a reactor.

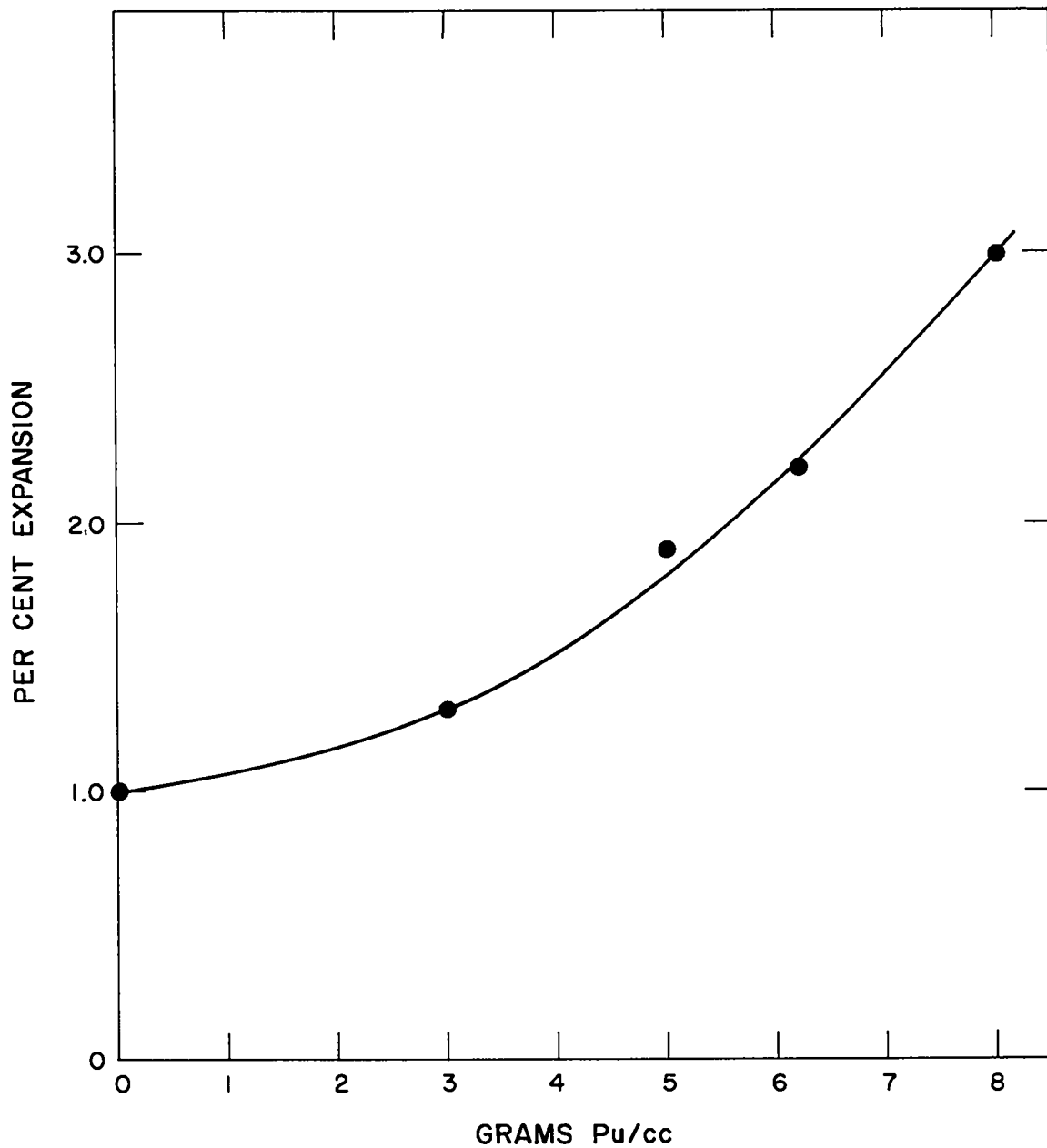


Fig. 4.1. Per Cent Expansion of Some Pu-Co-Ce Alloys on Freezing

of additives to the fuel, i.e., making the fuel a quaternary or higher order alloy. However, the additives which have been tried have not eliminated the problem. A second method is to employ a container of sufficient strength so that the fuel, rather than the container, will deform. Ta-5W alloys appear quite promising in this respect. The third potential solution is to avoid freezing the fuel. LAMPRE I was operated for some three years without allowing the fuel temperature to drop below the melting point of the Pu-Fe fuel (410°C).⁽²⁾ This is, however, an operational inconvenience.

Although molten Pu fuel has certain unique problems associated with its usage in power reactors, it also has certain advantages that cannot be attained by a solid fuel material. The fact that the fuel is in the molten state eliminates radiation damage problems with respect to mechanical properties of the fuel material. This problem, of course, is still important in reference to the container. There are two factors which may be expected to limit the life of the molten fuel in a reactor: chemical dilution and retained fission gases (Section 3). The first phenomenon, chemical dilution, might cause operational problems, such as

- (a) increased corrosiveness to the containment material,
- (b) alteration of the melting point (precipitation of solid phases thereby placing the fuel in a 2-phase state rather than in a single liquid phase),
- (c) changed physical properties (e.g., surface tension, which may affect the release of gaseous fission products).

The second problem, incomplete gaseous fission product release, would cause a gradual lowering of the density of the fuel and thereby cause operational difficulties (e.g., reactivity loss, accommodation of increased volume, etc.). It is clear that at the present time, the radiation effect, if any, which will limit the useful lifetime of a molten-fueled element in a reactor cannot be established. An attempt to determine what limits molten-fueled element performance is a prime objective of this experiment.

4.1 Container Alloy

4.1.1 Corrosion Performance

Considerable corrosion information is available on possible Ta alloy containment materials for use with Pu-Co-Ce fuels. Although in nearly all cases there are not enough samples at any single set of conditions (fuel composition, containment material, and temperature) to allow statistical analysis, certain conclusions may be drawn from the data available.

The results of tests carried out in Na environmental loops are summarized in Appendix E. It is evident there have been few failures. Tests involving fuels of 5-8 g Pu/cc in Ta containers have resulted in intergranular penetration of the container, all of these failures being associated with welds. Although intergranular penetration in this system has been rare, few tests have run more than 4200 hr, because many of the capsules have had to be removed from test because of damage on freezing (bulging and/or rupturing).*

In addition to the sodium loop tests, a large number of experiments have been performed in inert gas atmospheres (Appendix F). Test conditions covered a wide range of container materials and temperatures up to 850°C. Consideration of these data leads to the following observations:

- (a) All failures (except one 6.5 g Pu/cc fuel - Ta test) were associated with welds, predominantly the top seal weld.
- (b) There have been only two failures of Ta-10W alloy containers. These occurred at 850°C after 3500 and 4500 hr of testing, respectively. The failures were each 500 cpm in welds.
- (c) The addition of C to the fuel did not influence lifetime, even at 600°C.

* The Na loop test procedure involves operation for a given increment of time (e.g., 700 hr), each increment followed by a freeze and cold inspection of the capsules for leakage. Thus, capsules in this test program undergo a melt-freeze cycle for each test increment.

The following generalizations are drawn from these tests:

- (a) Pooling all Pu-Co-Ce alloy corrosion tests (all combinations of fuel composition, container material, and test temperature), it is observed that 136 tests have resulted in 27 failures of which 26 have been in welds. The one exception is the failure of Ta, 6.5 g Pu/cc, 3000 hr at 750°C (Appendix F). This failure was in the gas phase midway between the fuel level and the top seal weld.
- (b) When welds are removed from consideration, there is no clear indication of any temperature above which significant attack of Ta or Ta-W alloys occurs, for fuel compositions up to 8 g Pu/cc.
- (c) Although the number of capsules tested to determine the effect of carburization has been small, there is evidence to suggest an enhancement of corrosion resistance, probably by protection of seal welds below the fuel phase. (Results obtained with Pu-Fe fuel also support this contention.)
- (d) While no definitive trend with temperatures has been established, the present data are felt to be adequate to select a 700°C interface limit as being conservative.

The foregoing discussion has been concerned with presenting the available data regarding capsule lifetime based on IGP failures. In addition to this problem, the formation of a Ta-Co reaction layer may present problems, due to

- (a) spallation of Ta-Co (or Ta₂Co) precipitated layer, which could lead to mechanical mass transport and accelerated pitting-type corrosion, and
- (b) transport of Ta due to longitudinal thermal gradients in the capsules.

These two effects have both been demonstrated experimentally. Spallation of the Ta-Co layer has been observed in some tests; however, in many cases, i.e., Pu-Co-Ce fuels containing less than 5 g Pu/cc, the layer does not form in significant quantity below the liquid level within the times studied (up to ≈3000 hr). Fuels of 8 g Pu/cc do form Ta-Co intermetallic layers below the fuel level, whereas 6.2 g Pu/cc fuel appears to be borderline.

No pitting corrosion due to preferential Ta-Co layer spallation has been observed in tests thus far. However, tests at 1100°C of Pu-Fe fuel (which forms a similar reaction layer: Ta-Fe) have definitely indicated pitting and subsequent IGP through the container wall in the vicinity of the pit. In addition to allowing IGP, pitting decreases wall thickness, due to concentrated Ta solution effects and may form a hole completely through the container wall. (This type behavior may explain wall thinning and massive leakage observed in two LAMPRE I capsules. (2))

Thermal gradient mass transport of Ta has been demonstrated by tracer techniques. The maximum rate observed for a 100°C ΔT (600-700°C) with 5 g/cc Pu-Co-Ce is less than 0.1 mil/year. With 8 g Pu/cc fuel and a 100°C ΔT (650-750°C), the average rate of transfer of Ta was 0.19 mil/year. Mass transfer rates of these magnitudes should present little difficulty, providing that pitting is not initiated.

Preliminary work indicates the presence of a TaC layer on the container surface completely prevents Ta-Co intermetallic layer formation and may be self-healing. The carbide layer is established by bulk diffusion of C into the Ta and is not subject to spallation in thin layers (i.e., $<5 \mu$), although spallation of a portion of the layer has been observed with thick layers (i.e., 10-15 μ). Experiments using a temperature gradient of 100°C (600-700°C) with 5 g Pu/cc fuel and an initially uncarburized activated tab (at 700°C) contained in a carburized Ta capsule exhibited a Ta mass transport rate of 0.04 mil/year. It was observed that a TaC layer formed on the tab, and radioactive Ta was mass transported at only approximately half the rate obtained under equivalent conditions without the presence of a TaC protective layer. Because of the uncertainty associated with the Ta mass transport phenomenon and pitting corrosion, a carbide layer is specified for the reference capsule of the MPBE core, until and unless it can be proven by further experimentation that such a layer is not necessary.

4.1.2 Mechanical Properties

In addition to corrosion behavior, the mechanical properties of the container are important considerations in selecting a reference material. W additions to Ta have pronounced effects on hardness, ultimate and yield strengths, and percentage elongation. Table 4.1 shows selected properties at room temperature vs W content. Increasing W content of the alloy rapidly increases ultimate and yield strengths and moderately lowers percentage elongation. Mechanical property data presently available on Ta-W alloys are highly variable and unsatisfactory, making it necessary to generate additional data on potential capsule materials. Such a program is in progress.

Figure 4.2 shows yield strength of various Ta alloys vs temperature. The high temperature yield strength of Ta is markedly improved by W additions. Only one high temperature point is shown for Ta-5W; however, if it is assumed the temperature dependence of the Ta-5W curve is similar to that for Ta-10W, a factor of approximately seven should be obtained for Ta-5W yield strength over that of pure Ta at 750°C. If the results of tests in progress substantiate a yield stress of this magnitude for Ta-5W alloys ($\approx 42,000$ psi at 750°C), then all concern regarding capsule wall stress (Section 3.2) would be removed.

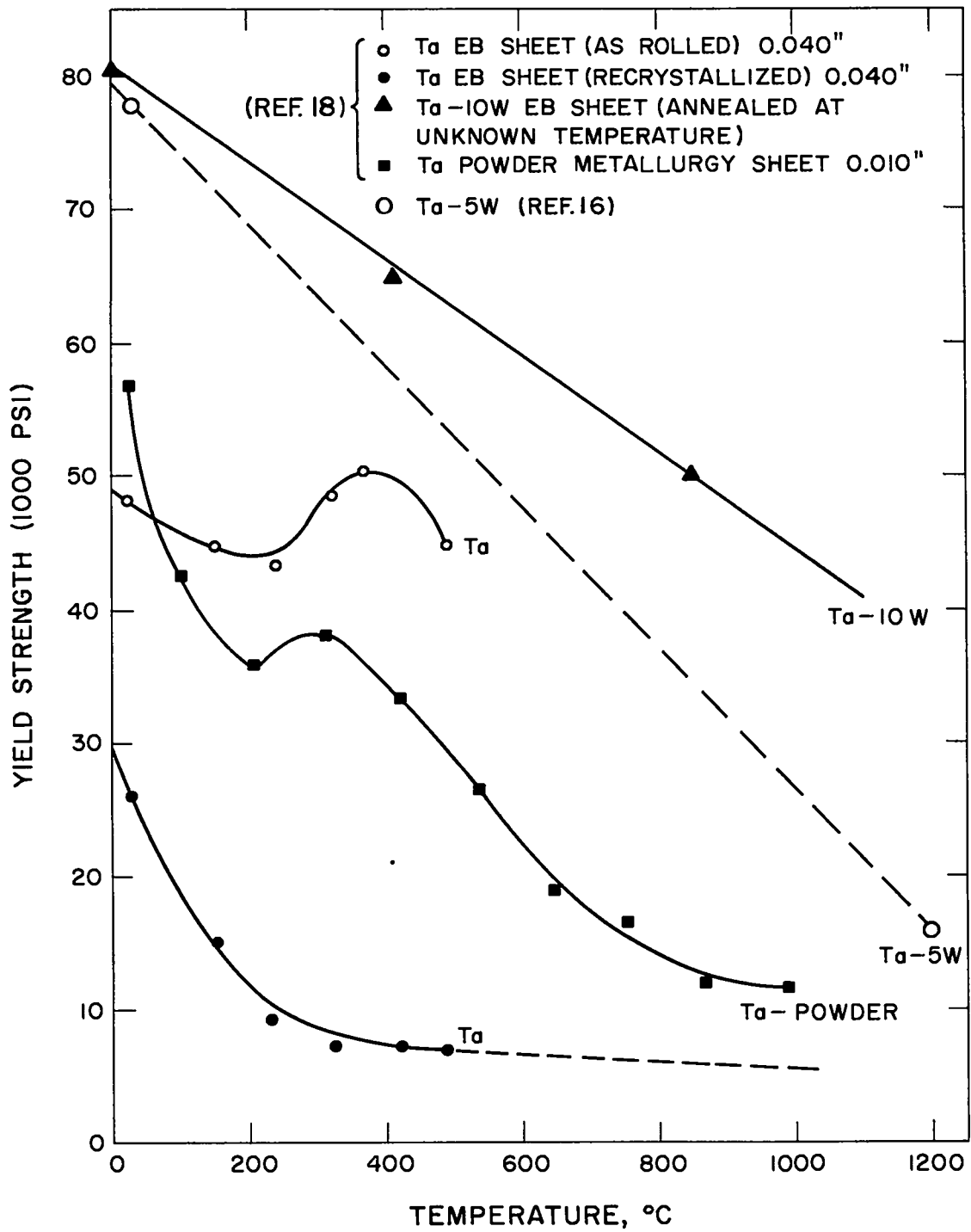


Fig. 4.2. Yield Strength (0.2% Offset) vs Temperature for Ta and Some Ta-5W Alloys

Table 4.1
Effect of W Additions on the Room Temperature
Mechanical Properties of Ta

<u>% W</u>	<u>Ultimate Tensile Strength</u>	<u>Yield Strength</u>	<u>% Elongation</u>	<u>References & Remarks</u>
1.5	45	35	40	Unpublished LASL Data
3.	55	40	32	(15)
5.	58.0	--	41	(15)
5.	84.0	78.5	19	(16)
7.	72	60	17	Unpublished LASL Data
10.	82.0	--	25	" " "
10	79.6	69.7	16	(15)
10	90	83	29	(17)
10	70-90	60-90	15-20	(18)
10	80	67	25	(19)
12.5	102	85-95	13 (arc cast)	
			23 (EB)	
15	89.0	--		

4.1.3 Irradiation Properties

Irradiation hardening increases the strength of Ta by two mechanisms: (1) transmutation $Ta^{181}(n, \beta)W^{182}$ and thereby burning in of W, and (2) fast neutron damage. Figure 4.3 shows results of transmutation of up to 3% W in Ta by neutron irradiation.⁽²⁰⁾ The neutron damage strengthening overshadows the W addition effect by a significant factor. Table 4.2 shows room temperature hardness values of Ta-10W alloy prior to and following neutron irradiation in a thermal flux at approximately 50°C. These data show, as expected, that at low irradiation levels, little irradiation hardening is obtained.

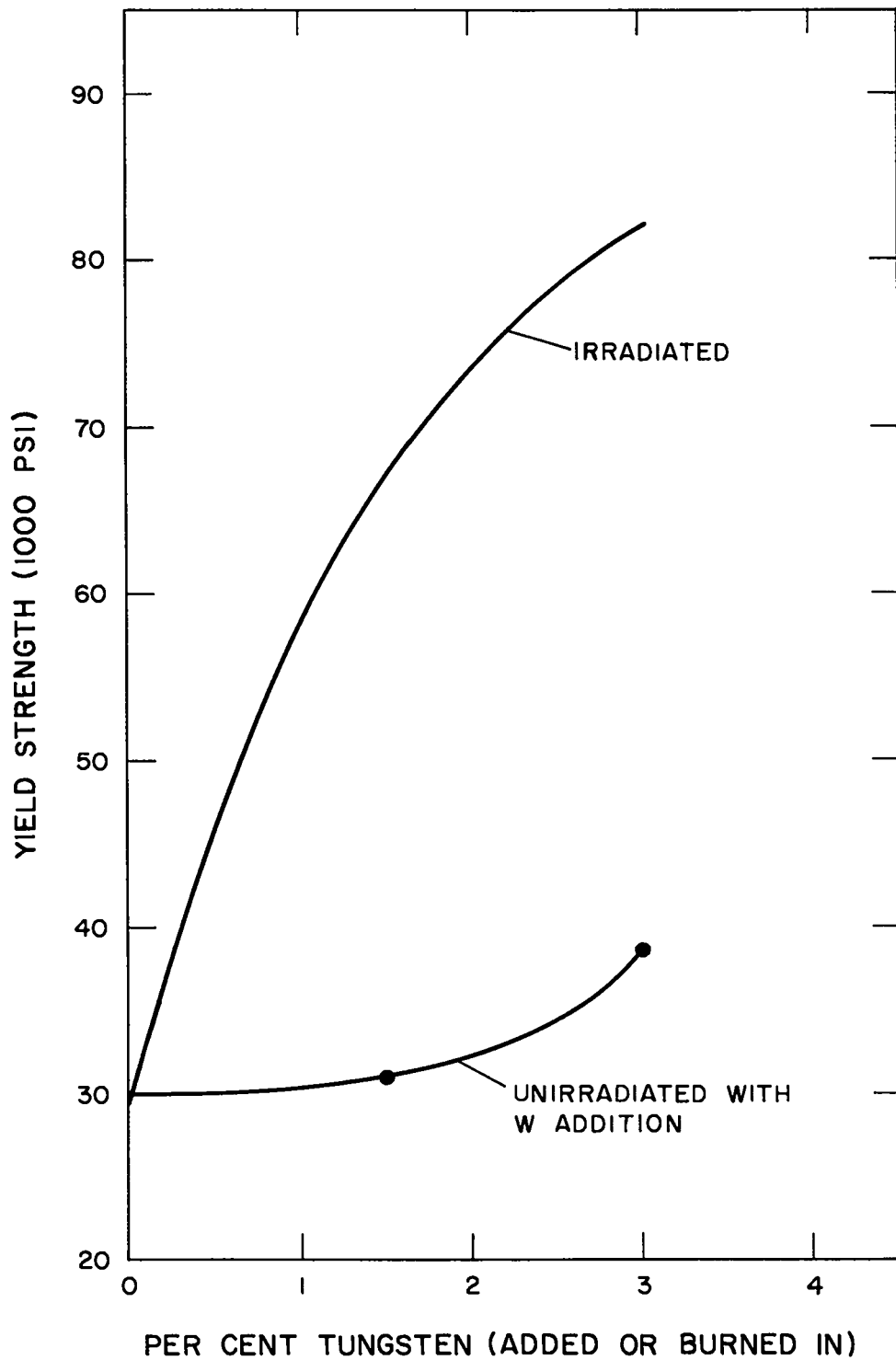


Fig. 4.3. Room Temperature Yield Strength of Irradiated Ta

Table 4.2

Effect of Irradiation on the Hardness^a of Ta-10W⁽²¹⁾

<u>Pre-Irradiation</u>	<u>Post-Irradiation</u>	<u>nvt</u>
67.0	68.1	8.8 x 10 ¹⁹
67.7	70.3	8.8 x 10 ¹⁹
68.5	61.4	1.02 x 10 ²⁰
67.6	69.5	1.02 x 10 ²⁰
68.3	68.1	1.02 x 10 ²⁰
67.9	70.0	1.5 x 10 ²⁰
66.8	70.3	"
68.3	69.7	"

^a Rockwell A scale, irradiated at ambient reactor temperature, tested at room temperature.

Post-irradiation hardness measurements have been obtained on Ta irradiated in LAMPRE I.⁽²²⁾ The results are shown in Fig. 4.4 and Table 4.3. The following observations are obtained from the data:

- (a) Transmutation of Ta to W was approximately a factor of 100 less for the LAMPRE I flux than for the MTR flux (specimens in Ref. 20 were irradiated in MTR). Since the hardness values for both types of irradiation environments are in excellent agreement (Fig. 4.4), the hardening appears to be due to a damage mechanism and not to W transmutation.
- (b) Since hardness values for 50°C irradiation in MTR flux agree quite well with the values obtained for irradiation between 500 and 600°C (0.24–0.27 of the absolute melting temperature, T_m), no annealing was obtained in LAMPRE I, and none should occur in MPBE.
- (c) Vacuum annealing for 1 hr at temperatures up to 900°C (0.36 T_m) did not markedly decrease the as-irradiated hardness.

The MTR data⁽²⁰⁾ indicate that the loss of room temperature ductility of Ta on exposure to 1.54×10^{21} nvt fast flux was 80% (from 35% elongation to 7%). However, the ends of the tensile specimens were

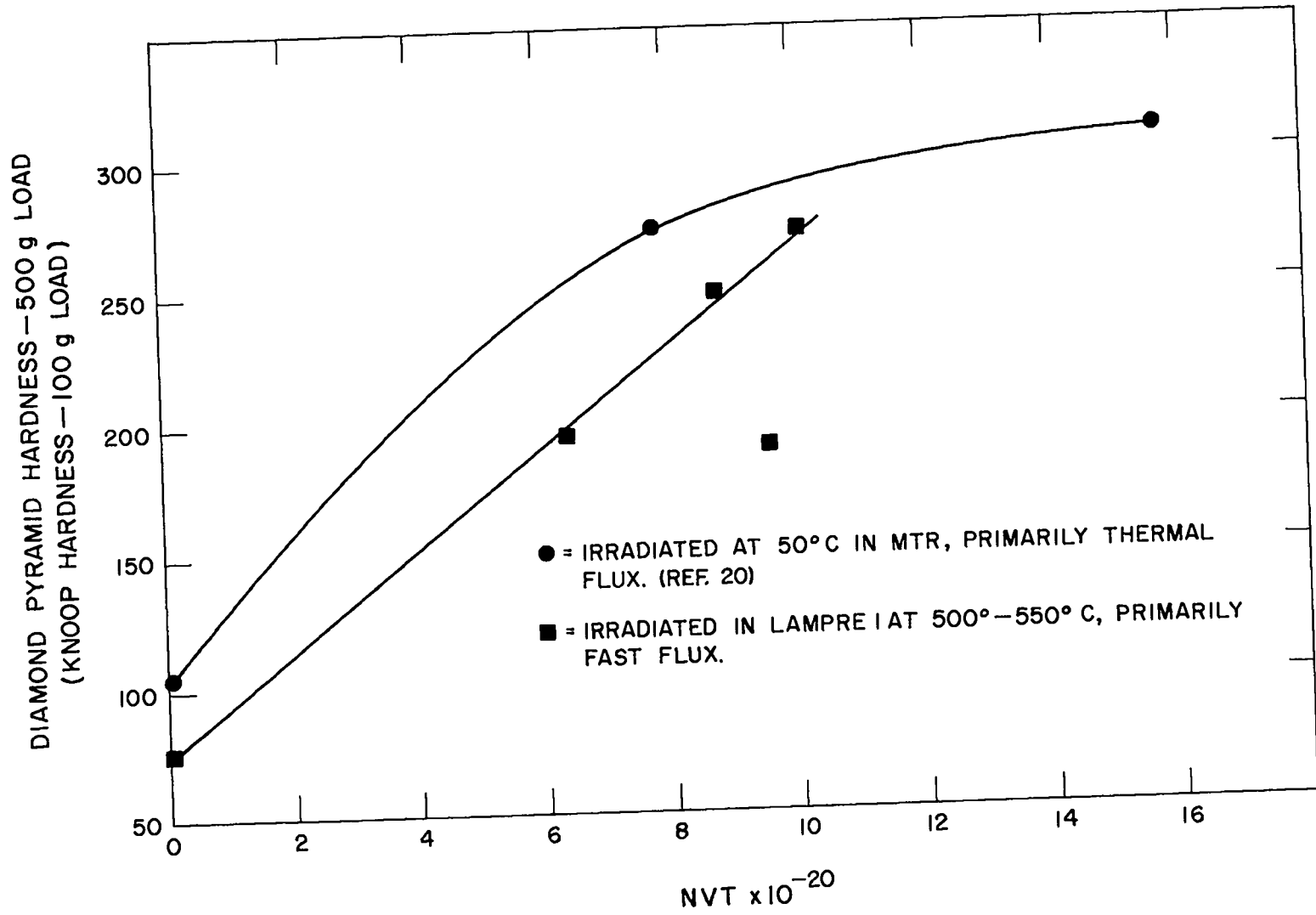


Fig. 4.4. Irradiated Hardness of Ta

Table 4.3

Hardness Data on LAMPRE End Caps

<u>Capsule</u>	<u>V_H as Irradiated</u>	<u>Anneal^a Temp. (°C)</u>	<u>V_H Post- Anneal</u>	<u>Calculated nvt (fast)</u>
1194	190	900	172	9.6×10^{20}
1294	273	800	261	10.2×10^{20}
1400	249	700	208	8.8×10^{20}
1597	195	600	176	6.4×10^{20}

^a 1 hr at temperature in vacuum.

subjected to bend testing by bending through 90° with one end clamped in a vise without any visual observation of crack formation. Even though these results indicate a retained ability to deform without fractures, these results must be viewed with caution, since a controlled radius of bend was not obtained during tests.

It appears from data available on Ta-W alloys that elongation decreases rapidly above about 12.5% W. If one accepts the hypothesis that a given percentage elongation is lost at a given nvt, it seems reasonable to maintain as high an unirradiated ductility as possible. Since it is expected that the elongation will decrease as Ta-W alloys are strengthened by increasing W content, a low W content, if consistent with adequate strength, is desirable. As a compromise, Ta-5W alloy has been selected as the reference fuel containment material.

4.2 Fuel Alloy

All parameters necessary for the selection of the ultimate fuel composition are not presently available. It is necessary, therefore, to have some flexibility built into the selection of fuel. In addition, the fuel composition selected for MPBE will be higher in Pu concentration than would be desirable for a large power reactor (Section 3.3). It would be valuable to have flexibility with respect to Pu composition so data generated in this experiment will be directly applicable to large core applications. The Pu-Co-Ce system has this flexibility.

Primary advantages of this system are:

- (a) Pu concentration is continuously variable from 0-13 g Pu/cc (Fig. 4.5).
- (b) Alloys covering this concentration range melt below 450°C.
- (c) Corrosion performance is superior, at any given temperature and container material, to other Pu alloys which have appropriate melting points.

While, for testing, it is desirable to use as high a Pu concentration in the fuel as possible (Section 3.2), data presented in Appendices E and F indicate a definite increase in corrosiveness to Ta with increasing Pu content of the fuel. Mass transport experiments also have indicated an increase in rate of Ta transport as the Pu concentration increases. All intergranular penetration observed with Pu-Co-Ce fuels to date has been associated with welds, and it is anticipated that the mechanical design of MPBE will not allow bulk amounts of fuel to come in contact with any welded metal (Fig. 4.6). However, in absence of many more thousands of hours corrosion testing, it must be postulated that if penetration of nonwelded metal ever occurs, it will occur more rapidly the higher the Pu concentration of the fuel. Based on these considerations, a 6.2 g Pu/cc reference fuel has been selected. Any fraction of the core can later be loaded with 8 g Pu/cc fuel, if the corrosion data obtained prior to loading warrants such a change.

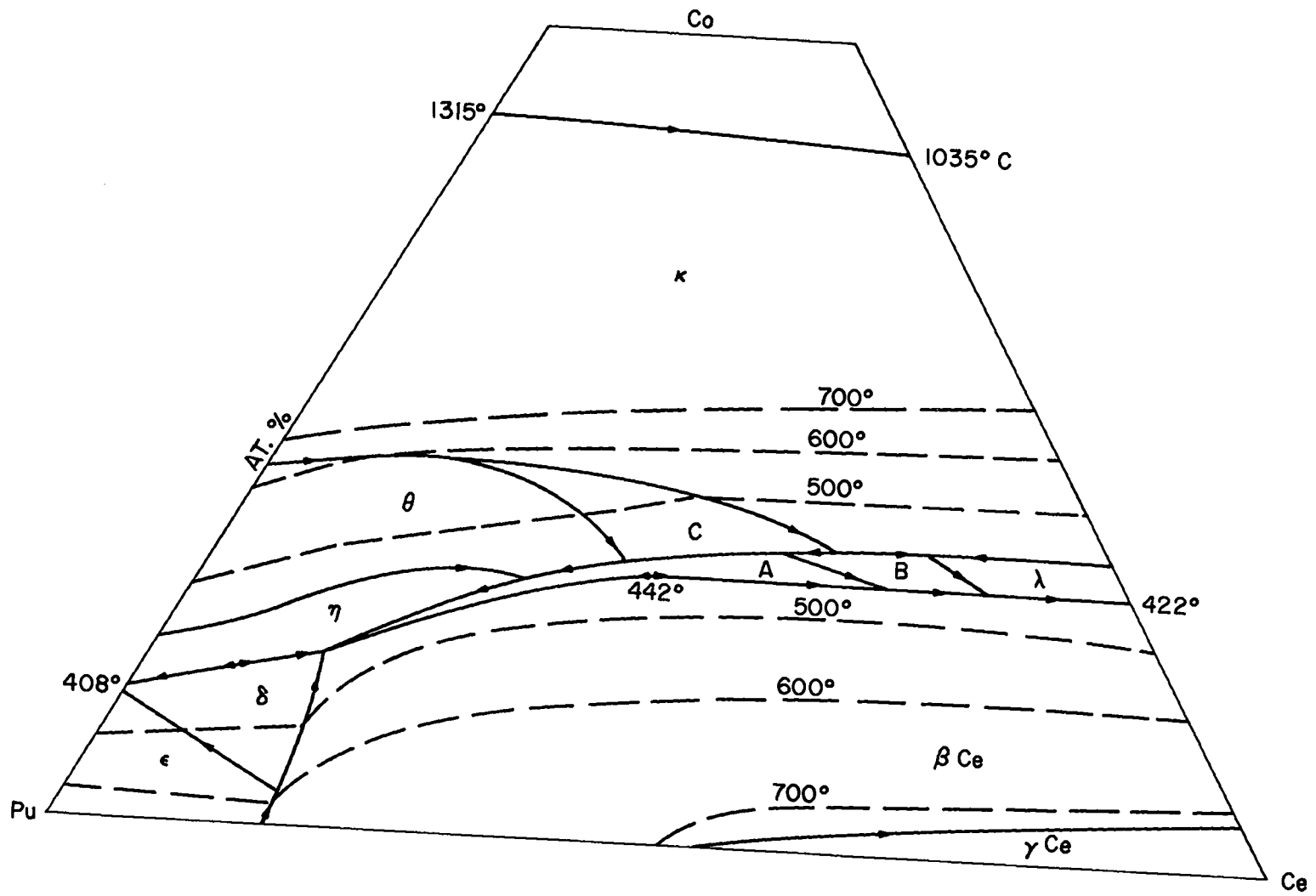


Fig. 4.5. Portion of Pu-Co-Ce Phase Diagram

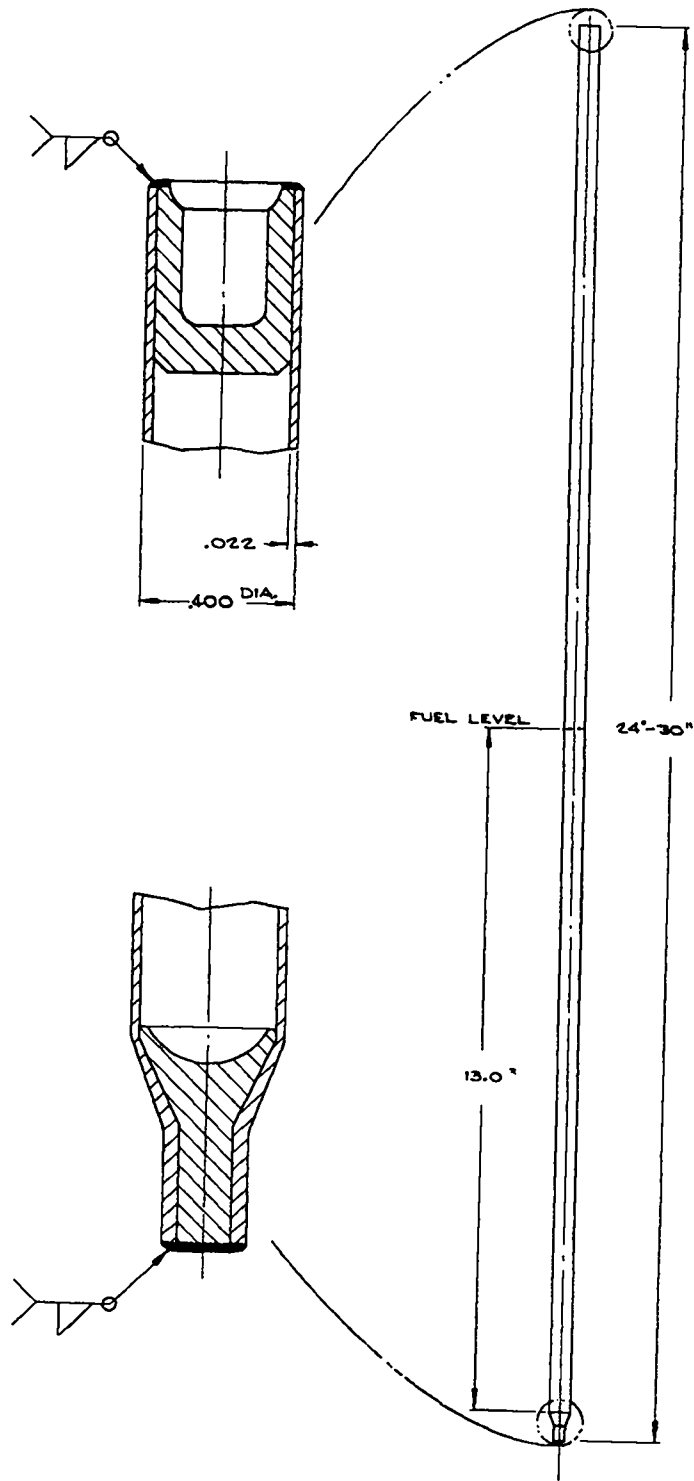


Fig. 4.6. MPBE Fuel Capsule Design

5. CORE DESIGN MODEL

The scoping studies, preliminary design studies, and nuclear design calculations described here have all utilized the two-dimensional S_n code (DDK).⁽²³⁾ The use of two-dimensional calculations at this stage is feasible only if the calculational model is held to modest size, both in detail and in extent. The availability of the DPC code,⁽²⁴⁾ however, has permitted the accounting for a considerable amount of detail in determining the material content of various regions in the design.

5.1 Region Compositions

In the descriptions in this section, all dimensions and compositions are 20°C values. Table 5.1 summarizes the effective compositions as used in the calculations.

5.1.1 Core

All core subassemblies are constructed of stainless steel cans in Na, each containing seven Ta capsules. Two distinct compositions fall in this category: fueled regions and gas-space regions, depending on the position of the region along the capsules. Figure 5.1 shows the cross section and dimensions of core subassemblies.

5.1.2 Reflector

Internal to the core sleeve are both fueled-core and core-reflector subassemblies. The reflector compositions may further be separated into axial reflectors (physically part of the fueled-core subassemblies, radial core-reflector subassemblies, and fueled-control

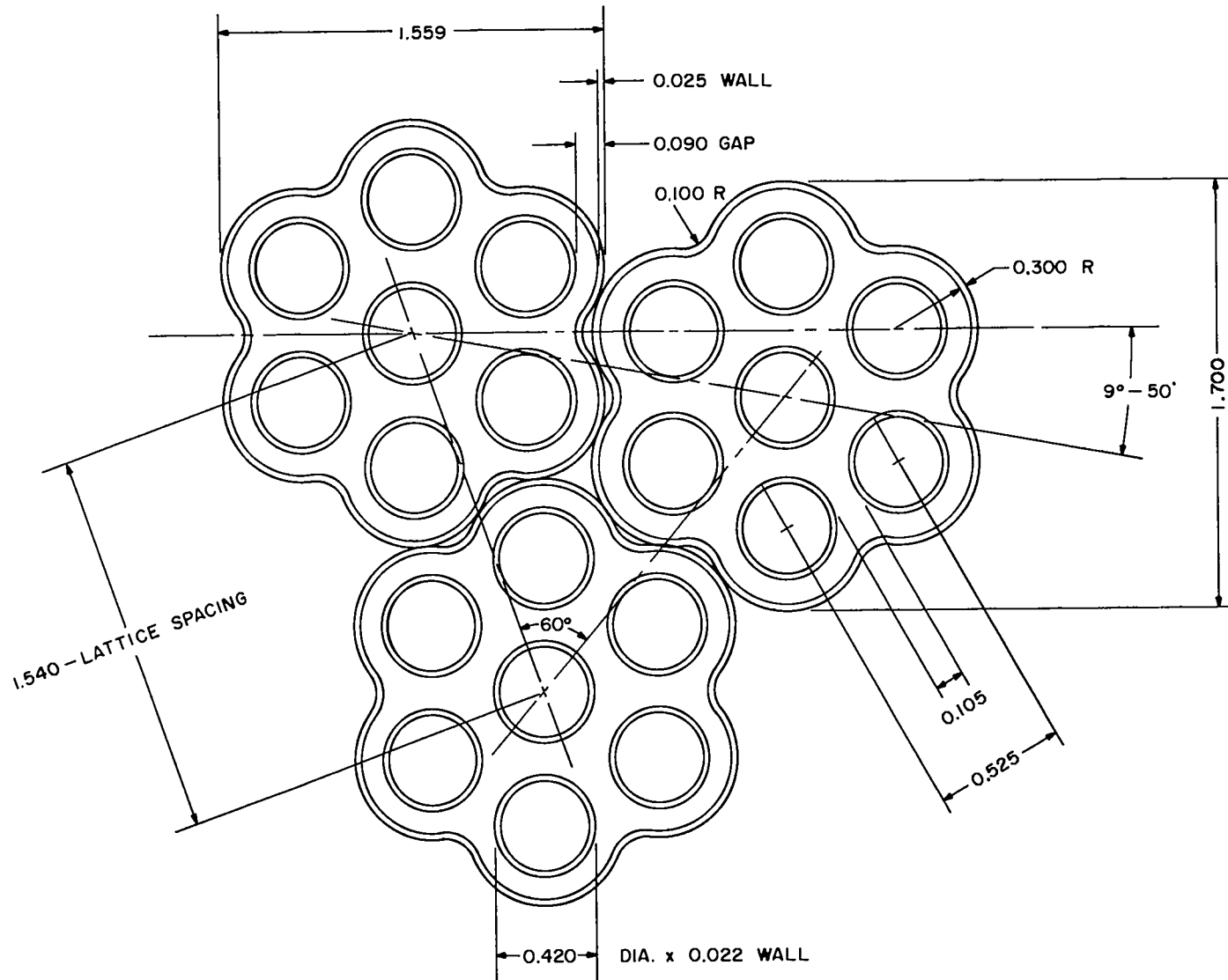


Fig. 5.1. Seven-Pin Corrugated Subassembly

followers (upper sections of fueled-control clusters). All have the same configuration as shown in Fig. 5.1 with the following exceptions. Rather than capsules, each contains seven solid rods. For axial reflectors, these rods are Ni, with the same diameter as the core capsules. For fueled-control followers, the rods are solid Ta, with the same diameter as the core capsules. The radial reflector rods are solid Ni of 0.500 in. diameter.

Table 5.1

Volume Fractions for Various Compositions
(v/o @ 20°C)

	<u>Na</u>	<u>SS</u>	<u>Fuel</u>	<u>Void</u>	<u>Ta</u>	<u>Ni</u>
Core	46.5	6.3	37.8	----	9.4	----
Gas Space	46.5	6.3	----	37.8	9.4	----
Axial Reflectors	46.5	6.3	----	----	----	47.2
Fueled-Control Followers	46.5	6.3	----	----	47.2	----
Margin	26.8	6.3	----	----	----	66.9
Control Segment, Ta	24.1	5.0	----	----	70.9	----
Control Segment, Ni	24.1	5.0	----	----	----	70.9
Structure (core sleeve, liner)	----	100.0	----	----	----	----
Ni Reflector	17.7	----	----	----	----	82.3
SS Thermal Shield	20.0	80.0	----	----	----	----

5.1.3 Control Segments

The control segment compositions are taken to include all of the material between the core sleeve and the core sleeve liner. As shown in Fig. 5.2, this includes spacers, Na, and the control segments proper. The dimensions are assumed to be as shown in Fig. 5.3. Two control segment compositions are considered: that with the control segment being Ni and that with Ta. In both cases, an extra 10% of the total region volume is assumed to be Na for internal cooling of the control segments.

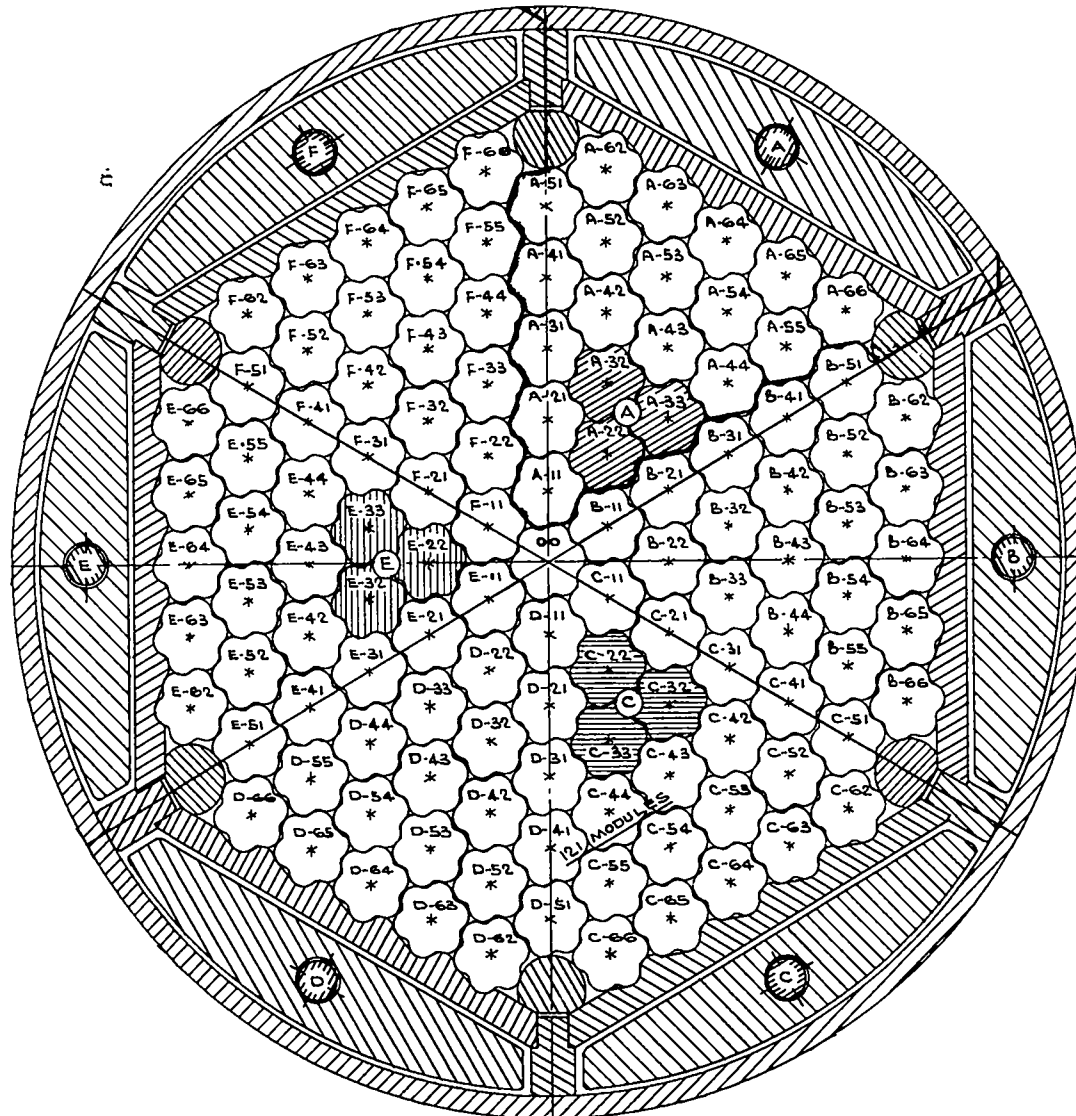
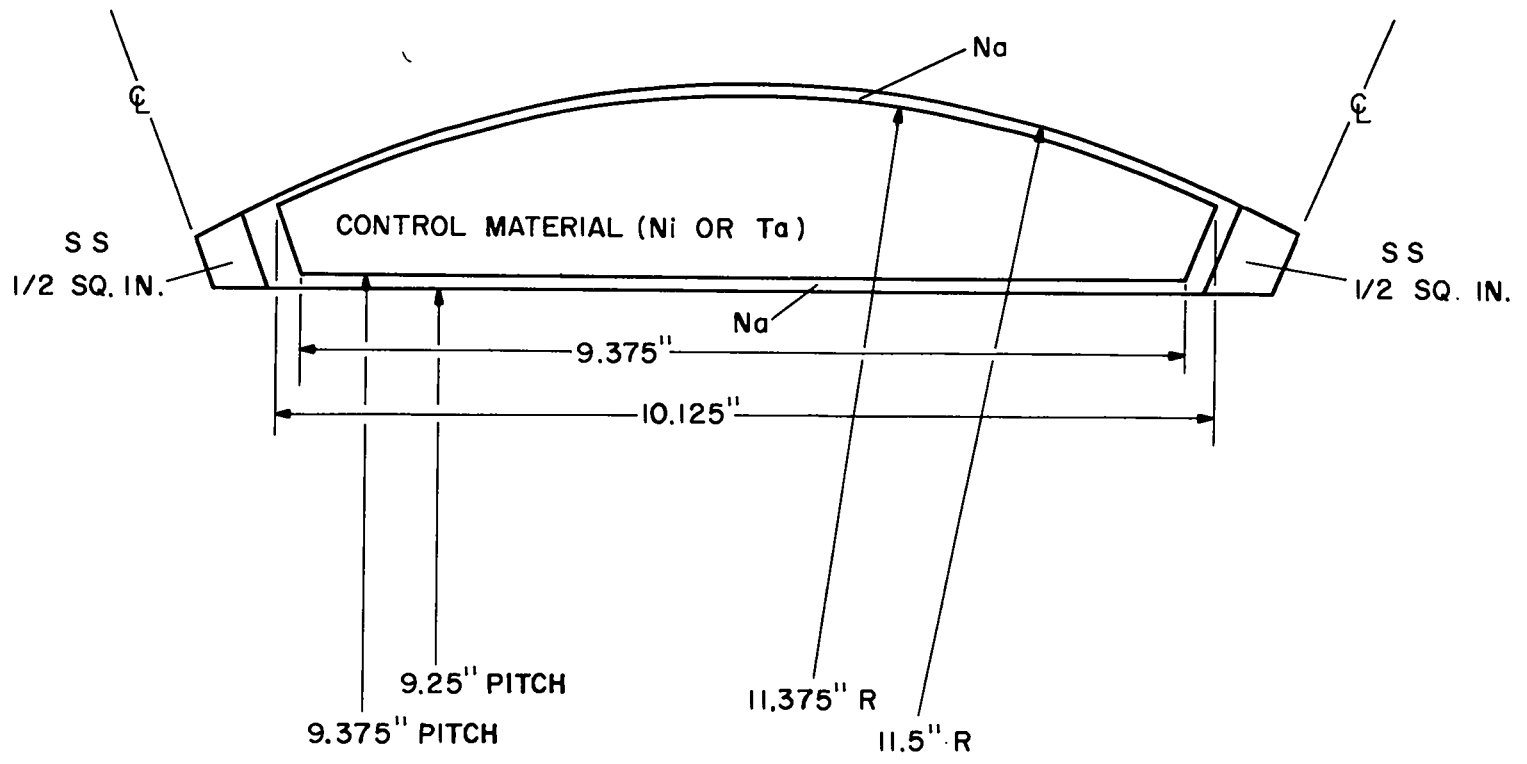


Fig. 5.2. Core Cross Section Used for Nuclear Design



47

Fig. 5.3. Control Segment Used for Nuclear Design

5.1.4 Structure

The core sleeve and core sleeve liner are described as being solid 304 stainless steel.

5.1.5 External

Two further compositions, both external to the core sleeve, are included in the calculational model: the Ni reflector and the stainless steel thermal shield. The reflector region is 82.3% Ni, 17.7% Na; the stainless steel thermal shield is 80% stainless steel, 20% Na.

5.2 Geometry

The general region layout shown in Fig. 5.4 has been used for all calculations considered here. This represents the preliminary design shown in Fig. 5.2. It will be noted that many of the engineering details present in the design are omitted from the calculational layout. When a region is described as containing a mixture of compositions, a volume homogenization is used. Further, it will be noted that all regions have been treated as cylinders.

In these calculations, the control configuration is represented in terms of the fraction of the control which is in the up position adjacent to the core. Since all regions in the calculation are cylindrical, any configuration in which either type of control is other than all-up or all-down has regions which are homogenizations of control-up and control-down compositions.

For the fueled-control clusters, the up position corresponds to alignment of the control clusters with their fixed counterparts, as will be essentially the case in practice. In the down position of the fueled-control clusters, the representation used is to extend the follower composition through the gas space; the gas space composition is placed in the control-core area; and the fuel composition is used in the control-reflector region. This does not preserve dimensions in general, but this approximation is small. A more significant approximation is that this travel corresponds to less motion than is presently anticipated for the facility

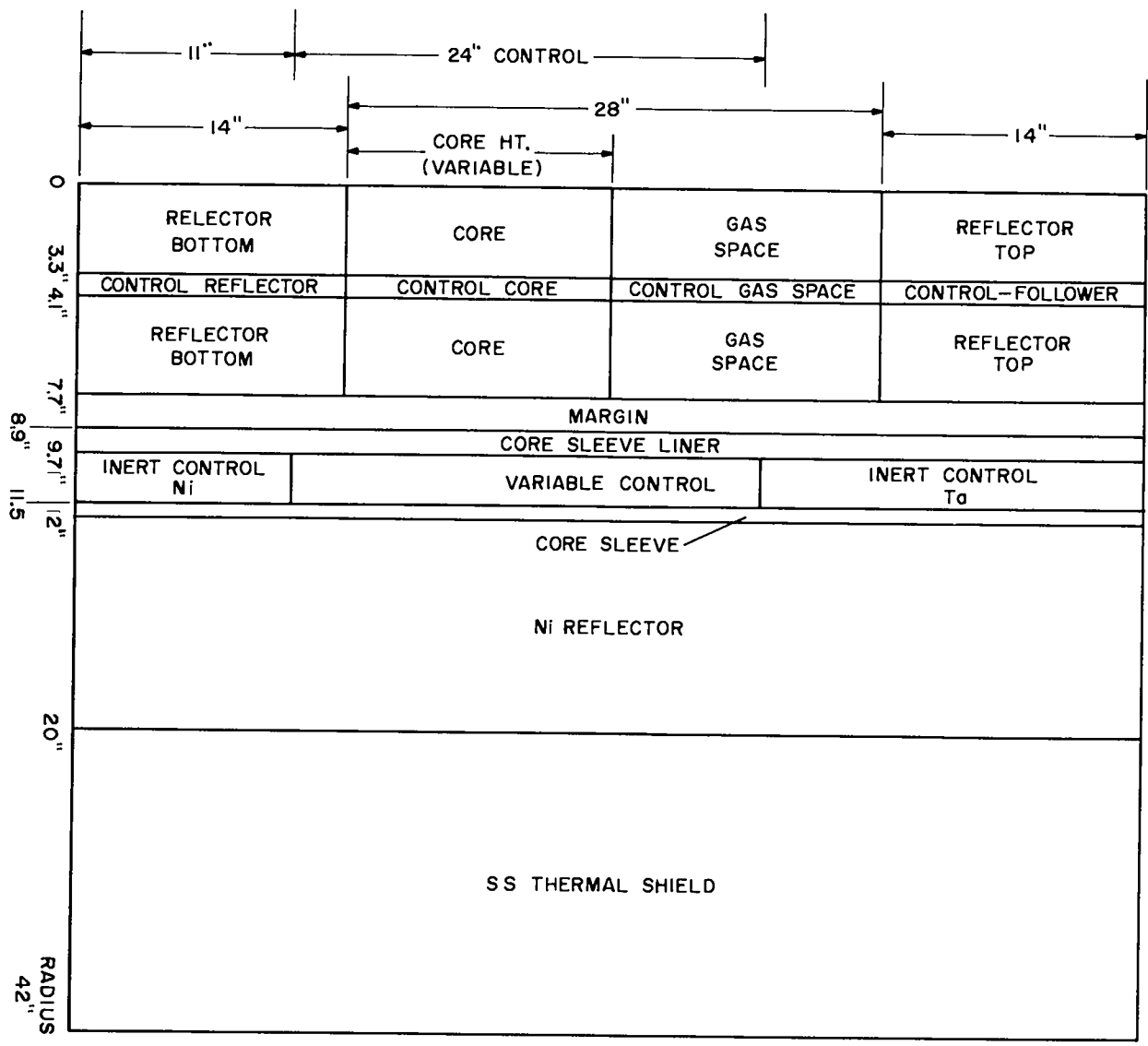


Fig. 5.4. MPBE Calculational Region Layout

(21 in.). Thus, the inferred fueled-control worths are conservative. For the (inert) control segments, the calculational stroke (24 in.) is more than in the design (21 in.), and the nominal position used is higher than it will be in the final configuration. With the extra travel, it is likely that the calculated worths are somewhat optimistic.

6. CALCULATIONAL RESULTS

Calculations have been done with this model to investigate critical loading and size, control worths, and reactivity coefficients. While these do not complete the required design calculations, they do describe the concept sufficiently to establish its applicability to the intended experimental program.

6.1 Critical Size and Loading

The core concept desired is to be adequate to handle fuel of either 6.2 or 8.0 g Pu/cc fuel. In addition, some margin in size is required for several purposes. Material requirements could call for the use of a lower Pu content fuel (Section 4). Augmentation of performance calls for higher Pu density fuel (Section 3). Beyond this, since this is a new fuel, a substantial margin for analytical uncertainty is advisable. Further, compensation for depletion by increasing size may be desired. Thus, a wide range of loadings may be of interest. Table 6.1 shows the estimated size and loading for a few cores.

Cases 92 and 95 are considered to be the reference cases. Case 98 represents a hot, just-critical case with the 6.2 g Pu/cc fuel. Case 10 is included as a measure of the minimum fuel density which might be tolerable in this core geometry without severely compromising the available gas space.

Table 6.1

Critical Size and Loading

Case	Fuel ($\frac{\text{g Pu}}{\text{cc}}$)	Temp. ($^{\circ}\text{C}$)	Fraction of		Number of Subassemblies	Loading		kg Pu
			Control Fuel	Up Inert		Height (in.) (@ 20 $^{\circ}\text{C}$)	Height (in.) (@ Temp.)	
92	6.2	530	2/3	1/2	91	13.2	13.3	95.8
98	6.2	530	2/3	2/2	91	11.6	11.7	84.7
09	6.2	160	3/3	2/2	91	11.2	11.3	81.4
95	8.0	530	2/3	1/2	91	8.4	8.4	79.3
10	5.0	530	2/3	1/2	121	16.0	16.1	124.2

6.2 Control Worths

If the final engineered control system is to be adequate for operational needs, then a preliminary model reactivity control swing of $\approx 5\%$ Δk from (fueled) control clusters and $\approx 5\%$ from (inert) control segments is advisable. However, since none of the operational requirements is well defined, the application of, or justification for, this control worth requirement is not well established.

Table 6.2 shows the calculated reactivity and reactivity swing for various control configurations.

For the 6.2 g Pu/cc, 530 $^{\circ}\text{C}$ cases, the following observations may be made: The total control swing (11.3% Δk) and the fueled control swing (7.3% Δk) both appear to be ample. The worth of the inert control segments is slightly less than might be desired (4.6%) but should be fully adequate. Some small interaction among various control motions may be inferred from the fact that the worths of fueled and of inert control do not add up to the combined worth. Part of this difference may be associated with the relatively loose convergence criteria used for these calculations.

Table 6.2
Control Worth Calculations

Case	Fuel (g Pu/cc)	Temp. (°C)	Fraction Control Up		k	Δk (%)	
			Fuel	Inert			
92	6.2	530	2/3	1/2	0.995	-----	
99A	↓	↓	0/3	0/2	0.924	-7.1	
98			3/3	2/2	1.037	+4.2	
99			0/3	1/2	0.946	-4.9	
98			3/3	1/2	1.019	+2.4	
94			2/3	0/2	0.971	-2.5	
93			2/3	2/2	1.016	+2.1	
02			160	2/3	1/2	1.008	-----
04			0/3	0/2	0.936	-7.2	
09			3/3	2/2	1.043	+3.5	
95			8.0	530	2/3	1/2	0.991
11	↓	↓	0/3	0/2	0.933	-5.8	
12			3/3	2/2	1.026	+3.5	
97			2/3	0/2	0.973	-1.8	
96			2/3	2/2	1.006	+1.5	

The control worths at 160°C are seen to be roughly comparable to those at 530°C.

For the 8 g Pu/cc fuel core, some loss in control worth may be noted. The fueled-control worth is not greatly reduced, in spite of the shortened stroke. The inert control is of somewhat more concern. This reduced worth is such as to suggest the possibility that different modes of operation may be required for the 8 g Pu/cc fuel case than for the 6.2 g Pu/cc fuel case, with somewhat greater reliance being placed on the fueled control.

6.3 Reactivity Coefficients

A few of the basic reactivity changes associated with normal changes in composition are given in Table 6.3. A considerable extension of this table, both from displacement and from perturbation calculations, is underway. It will be noted that none of these coefficients indicates serious difficulties.

Table 6.3

Reactivity Worth of Certain Changes

<u>Cases</u>	<u>Fuel</u>	<u>Change</u>	<u>Inferred Coefficient</u>
92-00	6.2	Isothermal ΔT	$-65 \times 10^{-6} \Delta k / ^\circ C$
92-13	"	Fuel-Expansion	$-3.6 \times 10^{-3} \Delta k / \%$ $-34 \times 10^{-6} \Delta k / ^\circ C$
92-05	"	Sodium Removal	$-4.7 \times 10^{-4} \Delta k / \%$ (uniform)
92-02	"	All Except Fuel Expanded	$-34 \times 10^{-6} \Delta k / ^\circ C$
92,04, 09,98	" "	Change in Fuel Height (constant density)	+0.33 $\Delta k / (\Delta H / H)$
02-92	"	Temperature Defect	-1.3% Δk
92-13	"	Power Defect (100°C)	-0.4% Δk
95-01	8.0	Isothermal ΔT	$-66 \times 10^{-6} \Delta k / ^\circ C$
95	"	Change in Fuel Height (constant density)	+0.30 $\Delta k / (\Delta H / H)$

6.4 Core Parameters

In addition to the results presented in Tables 6.1 through 6.3, Table 6.4 summarizes some of the design parameters for 6.2, 8.0, and 5.0 g Pu/cc fuel cores. The estimated performance figures are based on an assumed 20 MW(th) power. Figure 6.1 shows some calculated neutron power distributions.

Table 6.4

Summary of Some Properties of the Reference Cores

	g Pu/cc Fuel		
	6.2	8.0	5.0
Operational Loading (kg Pu)	95.8	81.5	124.2
Specific Power (kW/kg)	210.0	245.0	161.0
Power Density (MW/liter)	1.3	2.0	0.8
Minimum Critical Loading (kg)	84.7	-----	-----
Available Total Control Swing (% Δk)	11.3	9.3	-----
Available Fueled-Control Swing (% Δk)	7.3	-----	-----
Available Inert-Control Swing (% Δk)	4.6	3.3	-----
Power (peak/average)	1.46	1.43	1.50
Median Energy of Neutrons Causing Fission (MeV)	0.65	0.69	0.58
Median Flux Energy (MeV)	0.55	0.61	0.51
Average Flux (n/cm ² -sec)	1.7×10^{15}	2.0×10^{15}	1.3×10^{15}

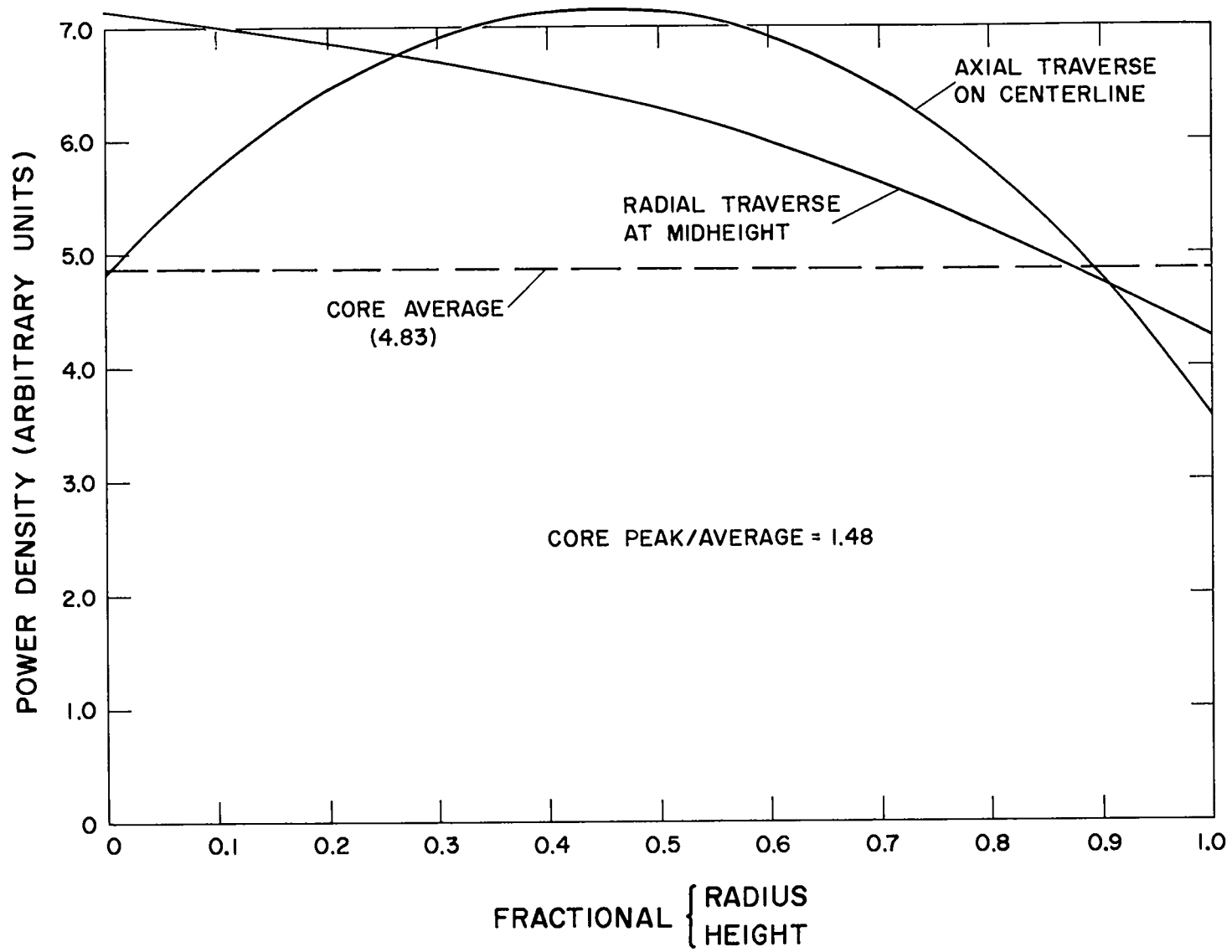


Fig. 6.1. MPBE Power Distributions

7. APPLICATION TO LARGE POWER REACTORS

In the context outlined above, it is of interest to consider the performance potential of a large, molten-Pu-driven, commercial fast breeder. It is not the intent here to present an accurate optimization, in that the system is still at the stage where it is not known what factors are limiting, let alone the limiting values for these parameters. Further, since little is known about performance of realistic blankets in this type of system, it is necessary to make some major assumptions.

The general configuration assumed is an array of reactor modules sufficient to produce 500-1500 MW(e) (typically 10-30 reactor modules). This modular arrangement allows a great degree of flexibility in obtaining performance data which can be extrapolated to large core sizes. Except for neutron leakage effects, a single module test would establish most of the basic performance properties of a large range of core sizes.

For each neutron leaking into the blanket (net), 1.2 neutrons are assumed to be captured in U-238. A small correction to the breeding ratios is used to account for fissile loss from 0.3% enriched U. No attempt is made here to calculate other than beginning-of-life breeding ratios and specific powers.

7.1 Core Parameters

It is assumed that the core is heat transfer limited. As described in Section 2, this assumption - without reference to the limiting value - is adequate to specify the Pu density in the fuel, which would be appropriate for any given capsule. This density will depend only on the

constants given in Eq. 2.3 (Section 2.2.3). For Ta capsules of the order of 1 cm diam, 0.02 in. wall, this yields a Pu density of 3-6 g Pu/cc fuel.

A specific realization, using various current best estimates for limiting factors, yields the parameters given in Table 7.1. Scaling of such a unit to a power range of commercial interest would involve an array including 10-30 such reactor modules [500-1500 MW(e) total, including blanket].

Table 7.1

Illustrative Figures for a Heat Transfer Limited Large Core

Doubling Time (core inventory)	7 yr
Breeding Ratio (beginning-of-life)	1.5
Specific Power (core inventory)	0.9 MW/kg Pu
Power Density	4.0 MW/liter fuel
Loading/Module	120.0 kg
Power/Module	110.0 MW(th)
Thermal Stress (in capsule wall)	10,000 psi
Maximum Wall Temperature	700°C
Fuel Density	4.5 g Pu/cc fuel
Capsule Size	0.4 in. o.d.
Capsule Wall	0.020 in. Ta

The results of a similar, but slightly different, set of assumed limits is shown in Fig. 7.1. In this case, it is assumed that mixed-mean Na coolant temperature rise, transverse temperature, and Na flow velocity are all fixed. Again, it is observed that a doubling time optimum is indicated for a Pu density in the 4-5 g Pu/cc fuel range. Another factor can be observed from this in a very qualitative way, in terms of the range of interest should a lower cross-section container be possible. Figure 7.2 shows the same data for the arbitrary selection of a fourfold reduction

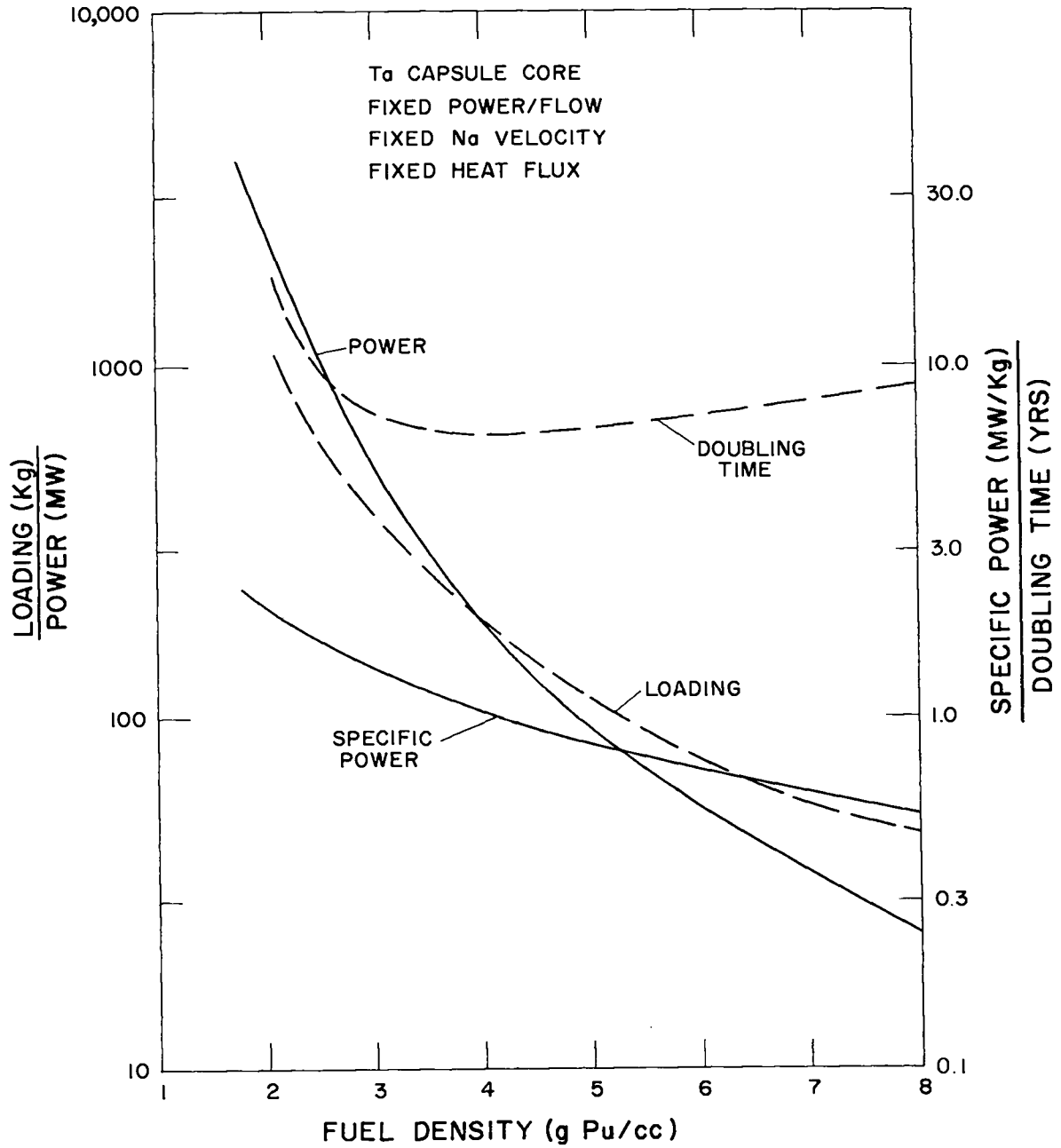


Fig. 7.1. Estimated Performance Factors - Large Molten-Pu-Ta Cores

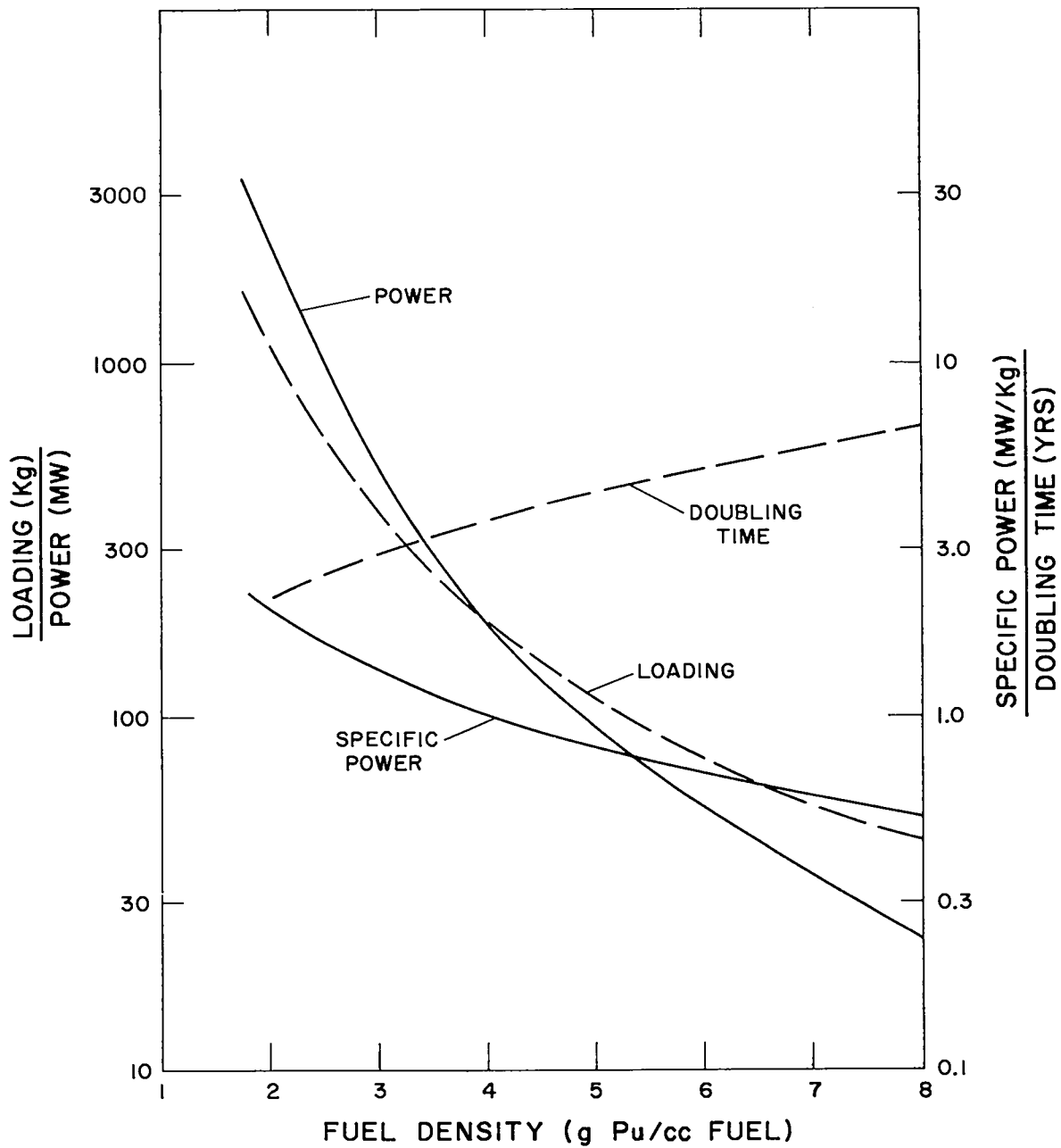


Fig. 7.2. Estimated Performance Factors - Reduced Parasitic Loss

in parasitic capture. It should be pointed out that the indicated range of interest (1-2 g Pu/cc fuel) is beyond the range of validity of the extrapolation, but the direction of the effect (toward large sizes) is correct. Further work is required to define a realizable optimum. The performance of such systems, if practicable, would be spectacular.

The other core parameters are somewhat less easily delimited at this stage. Depletion limits, as they affect core design, are unknown. Stress and temperature limits are uncertain, even for unirradiated materials, and the effects of a very hard spectrum irradiation are subject to many questions. But without unreasonable assumptions, acceptable performance estimates are available.

REFERENCES

1. E. O. Swickard, "The Los Alamos Molten Plutonium Reactor Experiment No. 1," Trans. ANS 2, 147 (1959); "LAMPRE I Final Design Status Report," LA-2833 (1962).
2. LAMPRE I Operations Report, in preparation.
3. W. H. Hannum, G. L. Ragan, and B. M. Carmichael, "An Application of Molten Plutonium Fuel to Fast Breeders," in "Proceedings of the Conference on Breeding, Economics, and Safety in Large Fast Power Reactors," ANL-6792, December 1963.
4. "A Preliminary Study of a Fast Reactor Core Test Facility," LA-2332, 1959.
5. "Guide to Nuclear Power Cost Evaluation," TID-7025, March 1962.
6. R. P. Hammond, R. E. L. Stanford, and J. R. Humphreys, Jr., "Mobile Fuel Plutonium Breeders," LA-2644, November 30, 1961.
7. "Large Fast Reactor Design Study," ACNP-64503, June 1964.
8. "Liquid Metal Fast Breeder Reactor Design Study," CEND-200, January 1964.
9. "Liquid Metal Fast Breeder Reactor Design Study," GEAP-4418, January 1964.
10. "Liquid Metal Fast Breeder Reactor Design Study," WCAP-3251-1, January 1964.
11. G. E. Hansen and W. H. Roach, "Six and Sixteen Group Cross Sections for Fast and Intermediate Critical Assemblies," LAMS-2543, November 1961.
12. R. M. Kiehn, "Some Applications of the S_n Method," NSE 4, 166, August 1958.

13. H. H. Hummel, K. Phillips, and A. Rago, "Calculation of Sodium Void Reactivity Effect for Large Fast Oxide Reactors in Spherical and Slab Geometry," in "Proceedings of the Conference on Breeding, Economics, and Safety in Large Fast Power Reactors," ANL-6792, December 1963.
14. J. H. Kittel, F. Sebilleau, R. G. Rateick, "Metallic Fuel Elements for Fast Reactors," ANS-100, April 1965.
15. R. H. Myers, "Some Properties of Tantalum-Rich Alloys with Wolfram and Molybdenum," Metallurgica, Vol. 42, pp. 3-9, 1950.
16. F. F. Schmidt, W. D. Klopp, E. S. Bartlett, & H. R. Ogden, "Investigation of the Properties of Tantalum and Its Alloys," WADD-TR-61-106, May 1961.
17. M. L. Torti, "Development of Tantalum-Tungsten Alloys for High Performance Propulsion System Components," NRC Report AD-275-158, 1960.
18. F. F. Schmidt and H. R. Ogden, "Engineering Properties of Tantalum and Tantalum Alloys," DMIC-189, September 13, 1963.
19. Stauffer Metals Division - Data Sheet.
20. C. K. Franklin, D. Stahl, F. R. Shober, D. F. Dickerson, "Effects of Irradiation on the Mechanical Properties of Tantalum," BMI-1476, November 18, 1960.
21. Quarterly Progress Report - Metallurgical Research Operation, Jan.-Feb.-March 1964, HW-81-269.
22. Unpublished Data, J. A. Basmajian, LASL.
23. B. G. Carlson, "Difference Equations in Neutron Transport Theory," Trans. ANS 6, 1, June 1963.
24. B. M. Carmichael and W. H. Hannum, "Two-Dimensional Data Preparation Code," in "The International Conference on the Application of Computing Methods to Reactor Problems," ANS, ANL, ENEA, May 1965.

APPENDIX A

DOUBLING TIME AND COSTING FACTORS

Consider a system with power capability of P MW operating at a load factor of ℓ , containing an inventory of M kg of fuel; and assume the system to be such that the inventory can be maintained at M kg fuel throughout the fuel cycle. Further, let the breeding ratio of the system (averaged over the fuel cycle) be BR atoms of fuel produced per atom of fuel lost. The rate of fuel loss is

$$\text{loss rate [g lost/day]} = (1 + \alpha) a_1 P \ell, \quad (\text{A.1})$$

where

α = capture-to-fission ratio of the fuel,

P = power in MW,

a_1 = grams fissioned/MWD,

ℓ = load factor.

The production rate is

$$\text{production rate [g produced/day]} = BR \times \text{loss rate.}$$

The doubling time (DT) is defined such that

$$DT [\text{days}] \cdot (\text{production rate} - \text{loss rate}) [\text{g/day}] = (M \cdot 10^3) [\text{g}] \quad (\text{A.2})$$

or

$$\begin{aligned} DT[\text{days}] &= \frac{10^3 [\text{g/kg}] M[\text{kg}]}{(\text{production rate} - \text{loss rate}) [\text{g/day}]} \\ &= \frac{10^3 M}{(\text{BR} - 1)(1 + \alpha) a_1 P \ell} , \end{aligned} \tag{A.3}$$

$$DT[\text{yr}] = \frac{10^3 M}{(\text{BR} - 1)(1 + \alpha) 365 a_1 P \ell} . \tag{A.4}$$

But $P/M = \text{SP}$ (specific power [MW/kg]), so

$$DT[\text{yr}] = \frac{2.74}{(\text{BR} - 1) \text{SP}(1 + \alpha) \ell a_1} . \tag{A.5}$$

For a fast breeder utilizing a very hard spectrum

$$a \approx 1 \text{ g fissioned/MWD},$$

$$\alpha \approx 0.1;$$

and taking

$$\ell = 0.83,$$

we have

$$DT[\text{yr}] \approx \frac{3}{(\text{BR} - 1) \text{SP}} . \tag{A.6}$$

To relate fuel charges to these factors, we may write the use charge as

$$\begin{aligned} U[\$/\text{MW-yr}] &= \frac{(\text{rate of interest})(\text{value of fuel})}{(\text{power production rate})} \\ &= \frac{(r)(\$)(M)}{(P)(\ell)} , \end{aligned} \tag{A.7}$$

where

$$r = \text{effective rate of interest [fraction/yr]},$$

$$\$ = \text{fuel value per kg}.$$

Thus

$$U[\$/\text{MW-yr}] = \frac{(r)(\$)}{(SP)(\ell)} . \quad (\text{A.8})$$

The buy-back, neglecting any reprocessing costs or losses, is

$$\begin{aligned} B[\$/\text{MW-yr}] &= \frac{(\text{Pu production rate} - \text{Pu loss rate})(\$)(10^{-3})(365)}{(P)(\ell)} \\ &= \frac{a_1 P(\text{BR} - 1)(1 + \alpha)(\$)(10^{-3})(365)(\ell)}{(P)(\ell)} \\ &= \frac{a_1}{2.74} (\text{BR} - 1)(1 + \alpha) . \end{aligned} \quad (\text{A.9})$$

The net fuel charge [per MW-yr]

$$\begin{aligned} U - B[\$/\text{MW-yr}] &= \frac{r}{(SP)\ell} - \frac{a_1(\text{BR} - 1)(1 + \alpha)}{2.74} \\ &= \frac{\$(\text{BR} - 1)(1 + \alpha)(a_1)r}{2.74} \left(\text{DT} - \frac{1}{r} \right) . \end{aligned} \quad (\text{A.10})$$

Using the above figures and

$$\$ = \$10^4/\text{kg},$$

$$r = 0.1 \text{ (10\%/yr)},$$

we have

$$\begin{aligned} U - B[\$/\text{MW-yr}] &= \frac{\$10^4(\text{BR} - 1)(1.1)(1)(0.1)}{2.74} (\text{DT} - 10) \\ &= (\$4)(10^2)(\text{BR} - 1)(\text{DT} - 10) . \end{aligned} \quad (\text{A.11})$$

There is thus a change in sign at $\text{DT} = 10$ yr, with zero net direct fuel charges (but not zero fuel cycle costs) at this value.

It may be noted that the incremental cost does not have the same functional form. Incremental costs correspond to a change in ℓ . In the above formulation, this appears as a change in net costs only through a

decrease in doubling time. This is necessarily a decrease in direct fuel cost, potentially of substantial magnitude. It is thus quite reasonable to anticipate very low total incremental costs (perhaps even negative). This is the basis for the attempts at obtaining a maximum plant availability consistent with other constraints.

It may also be noted that the breeding gain enters both directly and through the doubling time.

APPENDIX B

NEUTRON BALANCE

The general neutron balance of any critical system can be written

$$(\nu F)_f + (\nu F)_b = F_f + C_f + C_p + C_b + F_b + \ell, \quad (\text{B.1})$$

where

ν = neutrons born/fission,

F = fission rate,

C = capture rate,

ℓ = leakage rate,

and the subscripts

f denotes fuel,

b denotes fertile material,

p denotes other.

Breeding ratio (BR) is defined as fuel produced per fuel lost, or

$$\text{BR} = \frac{C_b}{F_f + C_f}, \quad (\text{B.2})$$

which, by (B.1) can be written

$$\text{BR} = \frac{\nu_f F_f + (\nu_b - 1) F_b - (F_f + C_f) - (C_p + \ell)}{F_f + C_f}. \quad (\text{B.3})$$

This may be written as

$$BR = \eta - 1 - a + b, \quad (B.4)$$

where

$$\eta = \frac{\nu_f F_f}{F_f + C_f};$$

$$a = \frac{C_b + \ell}{F_f + C_f}, \quad \begin{array}{l} \text{parasitic absorption, plus leakage per neutron} \\ \text{absorbed in fuel;} \end{array}$$

$$b = \frac{(\nu_b - 1) F_b}{F_f + C_f}, \quad \begin{array}{l} \text{net neutrons produced in fertile fissions per} \\ \text{neutron absorbed in fuel.} \end{array}$$

APPENDIX C

THERMAL PERFORMANCE RELATIONS

The following derivations are based on considering the detailed thermal behavior of a 1 cm height of a typical core cell, consisting of a fuel containing ρ_f [g Pu/cc fuel] in a capsule of material X of outside radius a [cm] and wall thickness b [cm]. The fuel generates fission heat at a rate SP [W/g Pu] which is transferred through the wall to a coolant. The heat flux HF [W/cm²], calculated at the average wall radius, induces a temperature difference through the wall of T_X and an associated thermal stress S_X .

Equating the heat generated to that transmitted, remembering that 1 cm height is being considered,

$$SP \text{ [W/g Pu]} \pi(a - b)^2 \text{ [cm]} \rho_f \text{ [kg Pu/cm}^3\text{]} = HF \text{ [W/cm}^2\text{]} \pi(2a - b) \text{ [cm]},$$

$$SP = \frac{2HF}{(a - b) \rho_f} \left[\frac{1 + b}{2(a - b)} \right]. \quad (C.1)$$

The ratio of the atom densities of wall material X to that of Pu is

$$\begin{aligned} \frac{N_X}{N_{Pu}} &= \frac{\pi(2a - b) b \text{ [cm}^2 \text{ X]} \rho_X \text{ [g/cm}^3\text{]}/A_X \text{ [g/mole]}}{(a - b)^2 \text{ [cm}^2 \text{ fuel]} \rho_f \text{ [g Pu/cm}^3 \text{ fuel]}/A_{Pu} \text{ [g/mole]}} \\ &= \frac{2C_1 b}{(a - b) \rho_f} \left[\frac{1 + b}{2(a - b)} \right], \quad (C.2) \end{aligned}$$

where

$$C_1 = \frac{\rho_X A_{Pu}}{A_X} .$$

Solving (C.2) for ρ_f ,

$$\rho_f = \frac{2C_1 b}{(N_X/N_{Pu})(a-b)} \left[\frac{1+b}{2(a-b)} \right] . \quad (C.3)$$

Using (C.3) in (C.1) yields

$$SP = \frac{HF}{C_1 b} (N_X/N_{Pu}) . \quad (C.4)$$

The temperature difference across the capsule wall is given by

$$T_X = \frac{HF [W/cm^2] (a-b) [cm] \left[\frac{1+b}{2(a-b)} \right] \left\{ \ln \left[\frac{a}{(a-b)} \right] \right\}}{k_X [W/cm^{\circ}C]} \quad (C.5)$$

where k_X is the thermal conductivity of material X. This may be approximated for thin-walled tubes, to first order in (b/a) , as

$$T_X \approx \frac{HF b}{k_X} . \quad (C.6)$$

The accompanying thermal stress is approximately

$$S_X [psi] \approx \frac{E_X [psi] \alpha_X [^{\circ}C^{-1}] T_X [^{\circ}C]}{2(1 - \nu_X)} \quad (C.7)$$

where E_X , α_X , and ν_X are the elastic modulus, linear thermal expansion coefficient, and Poisson ratio for material X.

If we define the constants

$$C_2 = \frac{1}{k_X} ,$$

$$C_3 = \frac{E_X \alpha_X}{2(1 - \nu_X) k_X} \quad (C.8)$$

we have

$$T_X = C_2 \cdot b \cdot HF, \quad (C.9)$$

$$S_X = C_3 \cdot b \cdot HF. \quad (C.10)$$

Some materials constants and resulting factors, as defined above, are given in Table C.1 for Ta. Also given are similar data for Nb, a material with better nuclear properties, though not necessarily acceptable as a container for Pu alloys. A_{Pu} is taken as 239 g/mole.

Table C.1

Selected Values of Some Physical Constants
and Defined Factors for Ta and Nb at 600°C

<u>Quantity</u>	<u>Units</u>	<u>Ta</u>	<u>Nb</u>
ρ_X	g/cm ³	16.40	8.46
A_X	g/mole	181.0	92.9
k_X	W/cm°C	0.682	0.653
E_X	10 ⁶ lb/in. ²	24.6	14.0
α_X	10 ⁻⁶ /°C	6.86	7.87
ν_X	none	0.35 ^a	0.38 ^a
C_1	g/cm ³	21.66	21.76
C_2	°C cm/W	1.466	1.531
C_3	psi cm/W	190.3	136.1

^a Room-temperature value

APPENDIX D

MEASURES OF IRRADIATION TIMES

Consider a reactor with effective one-group flux ϕ . The specific power (power per unit fissile material) is

$$SP \equiv \frac{\text{power}}{\text{loading}} \propto \frac{N_{\text{Pu}} \sigma_f^{\text{Pu}} \phi}{N_{\text{Pu}} \cdot V_{\text{Pu}}} = \text{const.} \cdot \phi \quad . \quad (\text{D.1})$$

The power density (power/unit fuel volume) is

$$PD = \frac{\text{power}}{V_{\text{Pu}}} \propto \frac{N_{\text{Pu}} \sigma_f^{\text{Pu}} \phi}{V_{\text{Pu}}} = \text{const.} \cdot N_{\text{Pu}} \cdot \phi \quad . \quad (\text{D.2})$$

The rate of burnup (per sec) is

$$N_{\text{Pu}} \sigma_a^{\text{Pu}} \phi \propto PD \quad . \quad (\text{D.3})$$

The fractional rate of burnup is

$$\frac{N_{\text{Pu}} \sigma_a^{\text{Pu}} \phi}{N_{\text{Pu}}} \propto SP \quad . \quad (\text{D.4})$$

The integrated dose to the fuel, measured in fissions/cc, is

$$\text{const.} \cdot \int PD \, dt \quad . \quad (\text{D.5})$$

The integrated dose to the container, measured in nvt, is

$$\int (nv)dt = \int \phi dt = \text{const.} \cdot \int SP dt \quad (\text{D.6})$$

or

$$\text{nvt (container)} = \text{const.} \cdot \text{fractional burnup.}$$

APPENDIX B

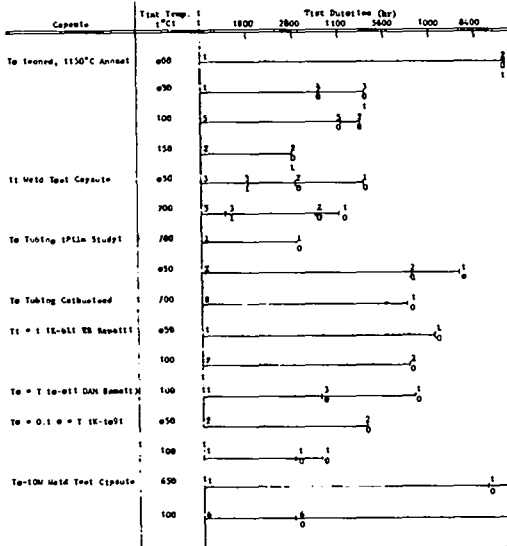
RESULTS OF Fe-Cr-ALLOY CORROSION TESTS
(IN A LOOP ENVIRONMENT)

EXAMINE LABORATORIES, S.A.S.

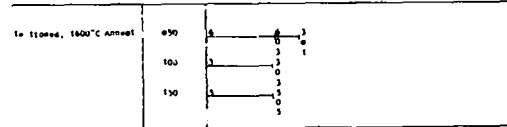
- A - No. of Capsules Tested
- B - No. that Failed Designated Test Definition
- C - No. that Failed at this Point Due to ICP
- D - No. that Failed at this Point Due to Rupture or Bulging



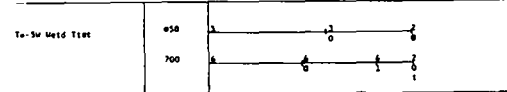
Test Concentration: 5 g Pu/lit



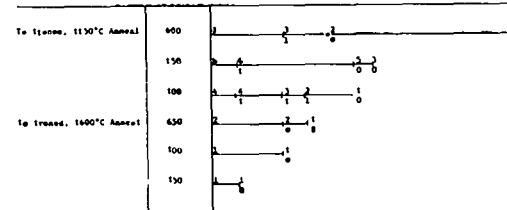
Test Concentration: 5.1 g Pu/lit



Test Concentration: 0.1 g Pu/lit



Test Concentration: 0.0 g Pu/lit



APPENDIX F

RESULTS OF Pu-Co-Ce ALLOY CORROSION TESTS
 STATIC LIQUID-GAS ENVIRONMENT

Legend: See Appendix E

